Gastroenterology 2015;149:981–992

MicroRNA214 Is Associated With Progression of Ulcerative Colitis, and Inhibition Reduces Development of Colitis and Colitis-Associated Cancer in Mice

Christos Polytarchou,[1] Daniel W. Hommes,[2,3,§] Tiziana Palumbo,[1,§] Maria Hatziapostolou,[1,§] Marina Koutsioumpa,[1] Georgios Koukos,[1] Andrea E. van der Meulen-de Jong,[2] Angelos Oikonomopoulos,[1,3] Welmoed K. van Deen,[2,3] Christina Vorvis,[1] Oksana B. Serebrennikova,[4] Eleni Birli,[1] Jennifer Choi,[3] Lin Chang,[5] Peter A. Anton,[6] Philip N. Tsichlis,[4] Charalabos Pothoulakis,[3] Hein W. Verspaget,[2] and Dimitrios Iliopoulos[1]

[1]Center for Systems Biomedicine, [3]Center for Inflammatory Bowel Diseases, Division of Digestive Diseases, [5]Gail and Gerard Oppenheimer Family Center of Neurobiology of Stress, [6]Center for HIV Prevention Research, David Geffen School of Medicine, University of California, Los Angeles, Los Angeles, California; [2]Department of Gastroenterology and Hepatology, Leiden University Medical Center, Leiden, The Netherlands; [4]Molecular Oncology Research Institute, Tufts Medical Center, Boston, Massachusetts

See Covering the Cover synopsis on page 829; see editorial on page 859.

BACKGROUND & AIMS: Persistent activation of the inflammatory response contributes to the development of inflammatory bowel diseases, which increase the risk of colorectal cancer. We aimed to identify microRNAs that regulate inflammation during the development of ulcerative colitis (UC) and progression to colitis-associated colon cancer (CAC). **METHODS:** We performed a quantitative polymerase chain reaction analysis to measure microRNAs in 401 colon specimens from patients with UC, Crohn's disease, irritable bowel syndrome, sporadic colorectal cancer, or CAC, as well as subjects without these disorders (controls); levels were correlated with clinical features and disease activity of patients. Colitis was induced in mice by administration of dextran sodium sulfate (DSS), and carcinogenesis was induced by addition of azoxymethane; some mice also were given an inhibitor of microRNA214 (miR214). **RESULTS:** A high-throughput functional screen of the human microRNAome found that miR214 regulated the activity of nuclear factor-κB. Higher levels of miR214 were detected in colon tissues from patients with active UC or CAC than from patients with other disorders or controls and correlated with disease progression. Bioinformatic and genome-wide profile analyses showed that miR214 activates an inflammatory response and is amplified through a feedback loop circuit mediated by phosphatase and tensin homolog (PTEN) and PDZ and LIM domain 2 (PDLIM2). Interleukin-6 induced signal transducer and activator of transcription 3 (STAT3)-mediated transcription of miR214. A miR214 chemical inhibitor blocked this circuit and reduced the severity of DSS-induced colitis in mice, as well as the number and size of tumors that formed in mice given azoxymethane and DSS. In fresh colonic biopsy specimens from patients with active UC, the miR214 inhibitor reduced inflammation by increasing levels of PDLIM2 and PTEN. **CONCLUSIONS:** Interleukin-6 up-regulates STAT3-mediated transcription of miR214 in colon tissues, which reduces levels of PDLIM2 and PTEN, increases phosphorylation of AKT, and activates nuclear factor-κB. The activity of this circuit correlates with disease activity in patients with UC and progression to colorectal cancer.

Keywords: IL6; IBD Progression; Mouse Model; Chronic Inflammation.

There is an increasing incidence of ulcerative colitis (UC), potentially resulting from the Westernized way of life, diet, and environmental alterations[1,2]; patients with long-standing and extensive disease are at increased risk of developing colorectal cancer.[3–5] Although early studies have shown standardized incidence ratios between 3.7% and 5.7%,[3,4] the magnitude of this risk is unknown. More recent studies have reported much lower rates most likely related to improved therapeutic management.[5–9] Practice guidelines recommend lifelong surveillance colonoscopies at intervals of 1–3 years, starting 8–10 years after diagnosis.[10] The rationale of surveillance colonoscopy is to detect premalignant mucosal dysplasia. Patients with high-grade dysplastic lesions are recommended to undergo prophylactic proctocolectomy, whereas for low-grade dysplastic lesions there is insufficient evidence to recommend surgery.[10] A medical decision analysis failed to show a benefit of surveillance colonoscopy, and, presently, there are also no clinical data to support the contention that surveillance colonoscopy is a cost-effective means to prevent death from colorectal cancer in UC patients.[11] Improving surveillance strategies with the use of molecular markers has not yet been successful. Markers associated with the dysplasia-cancer sequence have been reported, including aneuploidy,[12] p53,[13] microsatel lite instability,[14] and the

§Authors share co-authorship.

Abbreviations used in this paper: CAC, colitis-associated colon cancer; CD, Crohn's disease; CRC, sporadic colon cancer; IL, interleukin; miR, microRNA; mRNA, messenger RNA; PCR, polymerase chain reaction; qPCR, quantitative polymerase chain reaction; STAT3, signal transducer and activator of transcription 3; UC, ulcerative colitis; UTR, untranslated region.

Most current article

0016-5085/$36.00
http://dx.doi.org/10.1053/j.gastro.2015.05.057

mucin-associated sialyl-Tn antigen,[15] but none have yet been recommended in surveillance management. Genome-wide associated studies showed susceptibility loci and pathways that influence the risk of disease,[16,17] but alone are insufficient to determine specific causative relationships,[18] suggesting that other genetic and/or epigenetic alterations contribute to UC pathogenesis.[19]

MicroRNAs are small noncoding RNAs, 18–25 nucleotides in length, which regulate gene expression through binding in 3'-untranslated regions of target messenger RNAs (mRNAs).[20] MicroRNAs are essential regulators of inflammatory signaling pathways,[21,22] contributing to the pathogenesis of different human inflammatory diseases,[23–25] including IBD.[26,27] Furthermore, manipulation in the expression levels of microRNAs could suppress the inflammatory response,[24] suggesting their therapeutic potential. Although microRNA signaling pathways have been reported to link chronic inflammation to malignant transformation in breast cancer and liver cancer,[24,28,29] such evidence for UC-associated cancer currently is missing. We hypothesized that microRNAs may contribute to the development of UC and progression to colon cancer, while manipulation in the expression levels of these microRNAs could have therapeutic potential in patients with premalignant lesions.

Materials and Methods

Study Oversight

The study was approved by the institutional review board at each study center. All patients from whom tissue samples were obtained at the University of California at Los Angeles provided written informed consent. The patient samples were obtained at the Leiden University Medical Center according to the instructions and guidelines of the Leiden University Medical Center Medical Ethics Committee and in accordance with the Helsinki Declaration.

MicroRNA Library Screen

NCM460 immortalized epithelial cells were plated in 96-well plates and transfected with a microRNA inhibitor library consisting of 348 microRNA inhibitors and 2 negative control microRNAs (100 nmol/L) (Dharmacon, Inc, Lafayette, CO), as previously described.[27] At 24 hours after transfection, the cells were treated with interleukin (IL)6 for 24 hours, and the phosphorylation of nuclear factor-κB (NF-κB) was assessed by Phospho-RelA/NF-κB p65 (S536) Cell-Based Enzyme-Linked Immunoassay (KCB7226; R&D Systems, Minneapolis, MN). MicroRNA inhibitors that affected more than 50% of the phosphorylation of NF-κB were considered positive hits.

Statistical Analysis

All experiments were performed in triplicate unless otherwise stated. Statistical analyses were performed with the use of Origin software (version 8.6) (Origin Lab, Northampton, MA) and the SAS statistical package (version 9.4) (SAS, Cary, NC). The Student *t* test was used to examine the statistical difference in microRNA (miR)-214 expression between control colonic tissues and specimens derived from different intestinal pathologies, between active and inactive UC specimens, between UC specimens categorized based on disease duration, and between the differentially treated cells and mice groups. The Kruskall–Wallis test and the post hoc Wilcoxon 2-sample test with Bonferroni significance level adjustment for multiple testing were used for age comparisons, chi-square test was used for sex comparisons, and the Fisher exact test was used for tumor stage comparison. The correlation significance was determined by means of Spearman and Pearson correlation analyses. A P value of .05 or less was considered to indicate statistical significance.

Additional information is available in the Supplementary Materials and Methods section.

Results

High-Throughput Inhibition of the Human MicroRNAome in Human Colonocytes Shows Novel Regulators of NF-κB Activity

UC development is characterized by activation of inflammatory pathways, including NF-κB signaling. To identify microRNAs that regulate the NF-κB activity in human colonocytes, we performed a microRNA functional screen by targeting the human microRNAome in IL6-treated NCM-460 colonic epithelial cells (Figure 1*A*). In the primary screen, we found 9 microRNA inhibitors to regulate NF-κB phosphorylation levels by more than 50% ($P < 0.05$). Specifically, we found 2 microRNA inhibitors (miR-26b and miR-199a) that induced NF-κB phosphorylation levels significantly, and 7 inhibitors (miR-7, miR-146a, miR-373, miR-372, miR-181b, miR-21, and miR-214) suppressed NF-κB phosphorylation levels (Figure 1*B*). Among these inhibitors, previous studies have shown that miR-21, miR-181b, and miR-146a are essential regulators of the inflammatory response, validating our functional screen assay.[22,30] Interestingly, our screen showed that the inhibitor against miR-214 was the most efficient (>90%) suppressor of NF-κB phosphorylation, whereas the inhibitor against miR-199a was the most efficient (>90%) activator of NF-κB phosphorylation in human colonocytes.

MiR-214 Is Specifically Overexpressed in UC Colonic Tissues

According to our microRNA inhibitor screen data, in human colonocytes 7 microRNA inhibitors have the ability to suppress the inflammatory response significantly. Next, our aim was to evaluate the clinical relevance of these in vitro findings and to assess the expression levels of these microRNAs in human colonic tissues derived from UC and CD patients and control subjects (Figure 1*C*). Real-time polymerase chain reaction (PCR) analysis showed that miR-21 and miR-146a expression is increased in both UC and CD colonic tissues relative to controls, consistent with previous studies.[31] On the other hand, miR-7, miR-181b, miR-372, and miR-373 were not significantly deregulated in UC or CD relative to control subjects. Interestingly, we found that miR-214 is highly (>8-fold) up-regulated specifically in UC colonic tissues relative to control subjects and CD patient tissues. To further validate these findings in a large number of patient samples, we examined miR-214 levels in UC

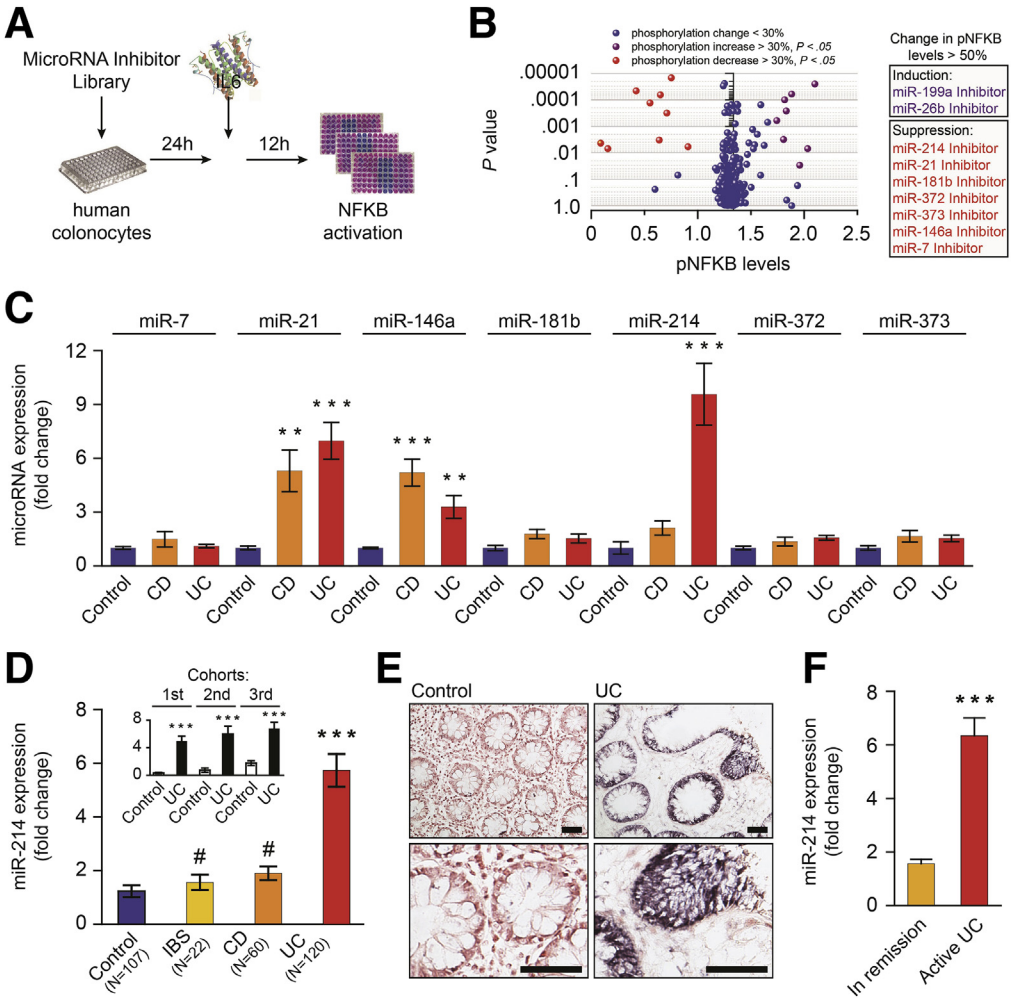

Figure 1. High-content inhibitor screening identifies microRNAs that control NF-κB in ulcerative colitis. (*A*) Screening workflow: a library of 348 microRNA inhibitors was transfected in colonic epithelial cells in triplicate and the activation of NF-κB was measured after treatment with IL6. (*B*) Screen data plotted as absolute levels (x-axis) of phosphorylated NF-κB (on S536), compared with scrambled sequence controls (no effect, value = 1.34) and *P* value from Student *t* test (y-axis). *Box* shows microRNA inhibitors that affect NF-κB phosphorylation by more than 50%. (*C* and *D*) MiR-214 is overexpressed specifically in colonic tissues from patients with UC. (*C*) MicroRNAs involved in the activation of NF-κB were quantified in colonic specimens by quantitative real-time PCR. (*D*) MiR-214 is overexpressed in colonic tissues from patients with UC from 3 different patient cohorts, as assessed by qPCR. IBS, irritable bowel syndrome; Data are represented as means ± SE. ***$P < .001$, **$P < .01$ in comparison with control; #$P < .001$, in comparison with UC, Student *t* test. (*E*) MiR-214 is up-regulated in the colonic epithelium of human active UC samples. In situ hybridization indicates the expression of miR-214 (blue) in the colonic epithelium of UC and control subjects. Nuclear Red was used as a counterstain. *Scale bars*: 50 μm. (*F*) MiR-214 expression correlates with UC activity. Data are represented as means ± SE. ***$P < .001$, in comparison with UC patients in remission, Student *t* test.

(n = 120) and control (n = 107) colonic tissues from 3 different cohorts (Supplementary Tables 1 and 2). Consistent with our initial findings, miR-214 levels were found to be increased significantly in UC, but not in irritable bowel syndrome (n = 22) or Crohn's disease (CD) (n = 60) (Figure 1*D*). In situ hybridization in human colonic tissues identified epithelial cells as the origin of miR-214 overexpression (Figure 1*E* and Supplementary Figure 1).

MiR-214 Expression Correlates With UC Disease Activity

To evaluate the clinical relevance of our findings, we examined miR-214 expression in correlation with different clinicopathologic parameters. MiR-214 levels were significantly higher in UC patients with active disease relative to patients in remission (Figure 1*F*), but did not differ in relation to UC patient sex or anatomic site, or to sex/disease location in CD patients (Supplementary Figure 2). Taken together, these results show that *MIR214* is an epithelial-expressed gene that regulates NF-κB activity and is deregulated specifically in UC in correlation with disease activity.

Integration of Computational and Molecular Analyses for Identification of miR-214 Downstream Targets in Colitis

To establish the molecular link between miR-214 and UC development, we aimed to identify downstream gene

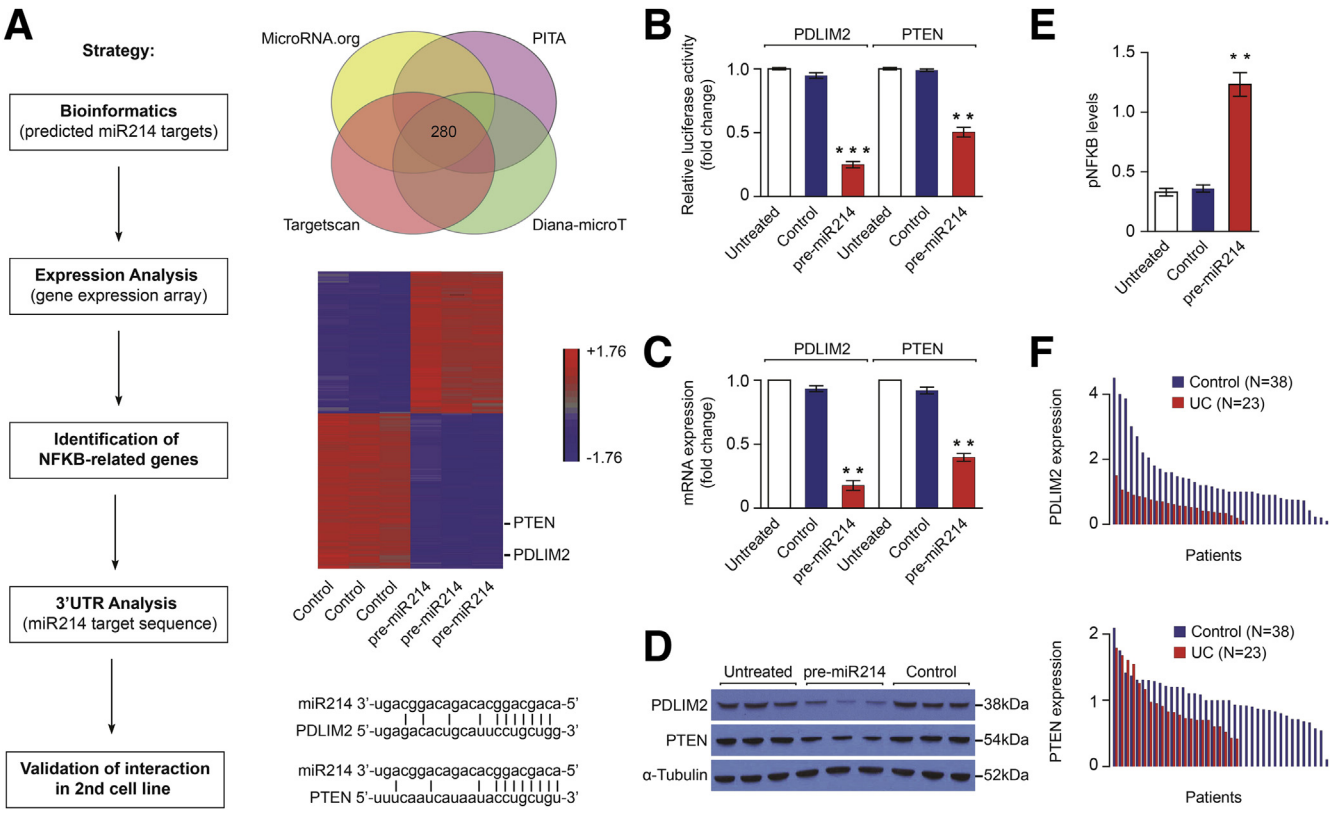

Figure 2. MiR-214 targets PDLIM2 and PTEN and activates NF-κB in the colonic epithelium. (*A*) Strategy for the identification and validation of miR-214 targets regulating NF-κB. MiR-214 targets predicted by 4 different types of software (n = 280). Gene expression analysis validated 71 miR-214 direct targets inhibited by more than 50% (**$P < .01$). Targets were sorted based on relation to the NF-κB pathway and alignment of the 3'UTR of mRNAs and the miR-214 sequence. (*B*) MiR-214 targets the 3'UTR of PDLIM2 and PTEN mRNAs. Luciferase assays performed in a second colonic epithelial cell line, NCM460, showed significant inhibition of the 3'UTR reporter activities by miR-214. Data are shown as the means ± SE. ***$P < .001$, **$P < .01$, in comparison with untreated and control (scramble) miR-treated cells, Student *t* test. (*C*) MiR-214 regulates the mRNA levels of PDLIM2 and PTEN in colonic epithelial cells. Effect of miR-214 on the expression of PDLIM2 and PTEN in NCM460 cells, as assessed by qPCR. Data are shown as the means ± SE. **$P < .01$, in comparison with untreated and control (scramble) miR-treated cells, Student *t* test. (*D*) MiR-214 regulates the protein levels of PDLIM2 and PTEN in colonic epithelial cells. Western blot analysis of PDLIM2 and PTEN protein levels in NCM356 from 3 independent replicates. α-Tubulin was used as loading control. (*E*) MiR-214 regulates the phosphorylation of NF-κB on S536. Data are shown as the means ± SE of phosphorylated nuclear factor-κB (on S536) levels, as assessed by ELISA. **$P < .01$, in comparison with untreated and control (scramble) miR-treated cells, Student *t* test. (*F*) PDLIM2 ($P < .01$) and PTEN ($P < .05$, Student *t* test) expression is down-regulated in colonic tissues from UC patients.

targets that could mediate NF-κB activation in human colonocytes. We developed an innovative strategy, consisting of 5 different steps, to identify the key effectors of miR-214 activity in UC (Figure 2*A*). Specifically, during the first step we used 4 different types of microRNA target prediction software and identified 280 common miR-214 gene targets based on their sequence complementarity. The second step was to analyze the expression of the genes regulated by miR-214 overexpression in human colonocytes, by performing high-throughput expression analysis. This analysis showed a signature of 71 genes (Supplementary Table 3) that were expressed differentially (expression, <50%; $P < .01$) in miR-214–treated NCM460 colonocytes. The next steps included evaluation of these 71 genes for their correlation with the NF-κB signaling pathway and direct interaction with miR-214 using 3' untranslated region (3'UTR) luciferase assays. Finally, these direct interactions between miR-214 and its target genes were validated in a second colonic epithelial cell line.

PDZ and LIM Domain 2 and Phosphatase and Tensin Homolog Are Direct Downstream Effectors of miR-214 in UC

The comprehensive analysis described earlier showed 2 genes that fulfill all the criteria as direct targets of miR-214 in UC. Specifically, PDZ and LIM domain 2 (PDLIM2) and phosphatase and tensin homolog (PTEN) were found to be expressed differentially in miR-214–overexpressing colonocytes, possessing target sequences for miR-214 in their 3'UTRs (Figure 2*A*). PDLIM2 is a nuclear ubiquitin E3 ligase and a known inhibitor of NF-κB activity,[32] and PTEN is a suppressor of the AKT signaling pathway[33] shown to intervene with NF-κB activation[34,35] and result in increased severity of colitis.[36] To validate the direct

interactions at the molecular level between miR-214 and PTEN or PDLIM2, we performed luciferase assays. Specifically, miR-214 was overexpressed in cells together with a luciferase vector harboring the 3'UTR of PTEN or PDLIM2 mRNAs. This analysis showed that miR-214 overexpression inhibited both PTEN and PDLIM2 3'UTR luciferase activities (Figure 2*B*). Furthermore, miR-214 overexpression suppressed PTEN and PDLIM2 mRNA (Figure 2*C*) and protein levels (Figure 2*D*). In addition, overexpression of miR-214 induced NF-κB (s536) phosphorylation (Figure 2*E*) and subsequently the expression of IL6 (Supplementary Figure 3), indicating that PTEN and PDLIM2 are direct downstream effectors of miR-214 involved in the regulation of the NF-κB inflammatory response. Finally, in reflection of the human relevance of these findings, PTEN and PDLIM2 mRNA levels were decreased in UC colonic tissues relative to controls (Figure 2*F*).

STAT3 Transcription Factor Regulates miR-214 Expression in Human Colonocytes

Given that miR-214 is up-regulated significantly in UC, we were interested to identify the molecular mechanisms that regulate miR-214 expression. We performed a bioinformatics analysis using the Lever/PhylCRM algorithm, which predicts highly conserved binding sites in promoter areas of genes.[37] This algorithm predicted that the strongest conserved binding site in the *MIR214* promoter area is for the transcription factor STAT3 (Figure 3*A*). To validate this prediction at the molecular level we performed a dual experimental approach. First, we performed

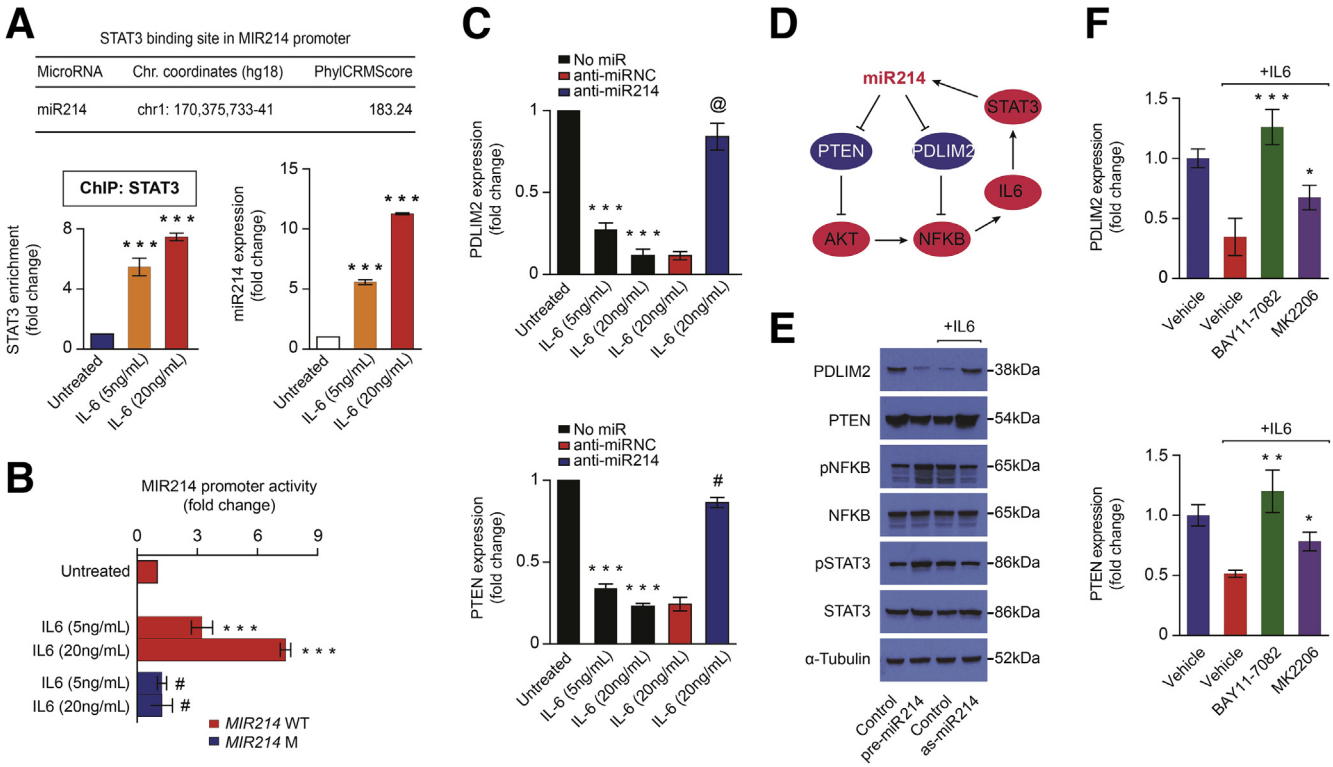

Figure 3. MiR-214 activates an inflammatory feedback loop circuit in the colonic epithelium. (*A* and *B*) Inflammatory signals transcriptionally activate miR-214 through STAT3. (*A*) The Lever and PhylCRM algorithms showed the presence of the STAT3 binding site on the promoter of the *MIR214* gene (*upper panel*). IL6 dose-dependently induces the binding of STAT3 on the promoter of the *MIR214* gene, as assessed by chromatin immunoprecipitation and qPCR analysis (*left panel*), and the expression of miR-214, as assessed by qPCR (*right panel*). Data are shown as the means ± SE. ***$P < .001$ in comparison with untreated cells, Student *t* test. (*B*) STAT3 binding on the promoter is required for the transcriptional activation of the *MIR214* gene. IL6 induces the luciferase activity of the wild-type (WT) *MIR214* gene promoter, whereas mutagenesis of the STAT3 binding site abolishes promoter activation by IL6. M, mutated STAT3 binding site. Data are shown as the means ± SE. ***$P < .001$ in comparison with untreated cells; $^{\#}P < .001$ in comparison with the IL6-induced WT promoter activity. (*C*) IL6 suppresses PDLIM2 and PTEN expression in colonocytes through miR-214. Effect of miR-214 inhibition on IL6-induced PDLIM2 and PTEN suppression, as assessed by qPCR. Data are shown as the means ± SE. ***$P < .001$ in comparison with untreated cells; $^{@}P < .01$ in comparison with negative control (NC) miR-treated cells, Student *t* test. (*D*) Schematic representation of the proposed model. (*E* and *F*) Activation and inhibition of the inflammatory feedback loop circuit. (*E*) miR-214 overexpression activates STAT3 while silencing of miR-214 abrogates the IL6-induced activation of STAT3. Western blot analysis of PDLIM2 and PTEN protein levels and the phosphorylation levels of STAT3 and NF-κB in NCM356 cells. α-Tubulin was used as loading control. (*F*) Pharmacologic inhibition of Akt or NF-κB reverses the IL6-induced suppression of PDLIM2 and PTEN, as assessed by qPCR. Data are shown as the means ± SE. ***$P < .001$, **$P < .01$, *$P < .05$ in comparison with IL6-treated cells, Student *t* test.

chromatin immunoprecipitation analysis by using an antibody against STAT3 and performed quantitative PCR (qPCR) upon stimulation with IL6, using primers specific for the *MIR214* promoter area. This experiment showed that STAT3 binds directly, in an IL6 dose-response rate, on the *MIR214* promoter. In agreement, qPCR analysis showed the IL6 dose-dependent induction of miR-214 expression (Figure 3*A*). In the second approach, the miR-214 promoter area was cloned in a reporter vector upstream of the luciferase gene. We found that IL6 induced *MIR214* promoter activity in a dose-dependent manner, an effect abolished by mutation of the STAT3 binding site (Figure 3*B*).

MiR-214 Is Part of a Feedback Loop Circuit Mediated by PDLIM2 and PTEN Genes

The role of miR-214 as an inflammatory mediator through the regulation of PDLIM2 and PTEN was studied in NCM356 human colonocytes. IL6 dose-dependently suppressed PDLIM2 and PTEN mRNA levels, an effect reversed by the inhibition of miR-214 (Figure 3*C*). In accord, Akt phosphorylation was increased upon IL6 treatment, and reduced by miR-214 inhibition (Supplementary Figure 4). These findings suggest that IL6 induces miR-214 through STAT3-mediated transcriptional activation, creating a positive feedback loop circuit (Figure 3*D*). Specifically, miR-214 overexpression directly suppresses the expression levels of *PTEN* and *PDLIM2* genes. The suppression of PDLIM2 results in direct activation of NF-κB, whereas the suppression of PTEN results in the activation of the AKT kinase, contributing to the phosphorylation of NF-κB. In turn, the NF-κB transcription factor induces IL6 expression and thus activates the STAT3 transcription factor, which binds directly on the *MIR214* gene promoter area, re-enforcing its up-regulation. To assess the activity of the feedback loop circuit we either overexpressed the microRNA or treated cells with IL6 in combination with miR-214 silencing. Western blot analysis of cell lysates collected 96 hours later showed the sustained suppression of PTEN and PDLIM2 and increased phosphorylation of NF-κB and STAT3 upon miR-214 overexpression or treatment with IL6. Importantly, miR-214 targeting reversed the effects of IL6, in support of the dependence of circuit activation on miR-214 (Figure 3*E*). Along the same line, pharmacologic inhibition of Akt or NF-κB resulted in partial or complete reversal, respectively, of the IL6-induced effects on PTEN and PDLIM2 expression (Figure 3*F*).

Effects of a miR-214 Chemical Inhibitor on UC Ex Vivo and In Vivo

To evaluate the therapeutic potential of miR-214 inhibition in UC through regulation of the feedback loop circuit, we used a chemically stable inhibitor that was highly efficient in suppressing miR-214 in human colonocytes in vitro (Figure 4*A*). We studied the effects of the miR-214 chemical inhibitor ex vivo on freshly isolated colonic biopsy specimens from UC patients with active disease (Figure 4*B*). The inhibitor efficiently inhibited miR-214 in the colonic explants (Figure 4*C*), and suppressed the inflammatory response by increasing the expression of both PDLIM2 and PTEN in colonic explants from 3 UC patients with active disease (Figure 4*D*). In addition to the ex vivo findings, we examined the effects of the miR-214 inhibitor on experimental colitis in mice. Mice treated with dextran sulfate sodium (DSS) and the miR-214 inhibitor and colitis disease activity was evaluated by using different parameters (Figure 4*E*). Importantly, we found that the miR-214 inhibitor reduced disease activity in DSS-induced experimental colitis (Figure 4*F*). Taken together, these in vitro, in vivo, and ex vivo data suggest the therapeutic potential of the miR-214 inhibitor in UC patients with active disease.

MiR-214 Is Overexpressed in Long-Lasting Colitis and Colitis-Associated Colon Cancer

Although the association between UC and colorectal cancer was documented as early as 1925,[38] its molecular biology remains to be explored. We questioned the role of miR-214 during the transition from UC to cancer. Interestingly, we found that miR-214 is up-regulated in mice with chronic but not acute inflammation induced by DSS (Figure 5*A*). In the same line, colonic tissues from patients with long-standing (>10 years) UC have increased miR-214 levels compared with colonic tissues from patients with UC for fewer than 10 years (Figure 5*B*), suggesting that miR-214 may provide a link between UC and colorectal cancer development. Notably, miR-214 levels do not change significantly in colonic tissues of 2,4,6-trinitrobenzenesulfonic acid–treated mice as well as in polyps formed in the adenomatous polyposis coli mutant (APC^{min}) mouse model (Supplementary Figure 5). Therefore, we compared miR-214 levels by qPCR and in situ hybridization in tumors from colitis-associated colon cancer (CAC) and sporadic colon cancer (CRC) patients. This analysis showed a dramatic overexpression of miR-214 in CAC, but no difference between CRC and controls (Figure 5*C* and *D* and Supplementary Figure 6). Overall, these findings suggest that miR-214 is increased during UC development and amplified during progression to colorectal cancer.

MiR-214 as a Novel Oncogene in Colon Cancer

To examine the significance of miR-214 in colorectal oncogenesis we performed gain-of-function and loss-of-function studies. Overexpression of miR-214 induced the colony formation ability (Figure 6*A* and Supplementary Figure 7*A*) and invasiveness (Figure 6*B* and Supplementary Figure 7*B*) of human colon cancer cells, suggesting its oncogenic role. On the other hand, silencing of miR-214 suppressed the IL6-induced tumorigenic and invasive phenotype, pointing to the dependence of IL6 tumorigenic effects on miR-214. Next, we investigated whether miR-214 acts through regulation of the feedback loop circuit. We found that IL6 up-regulated miR-214 in HCT-116, HT-29, LoVo, and DLD-1 colon cancer cells (Figure 6*C*), mediated by the direct binding of STAT3 on *MIR214* promoter area (Figure 6*C* and *D*). Furthermore, IL6-induced miR-214 expression resulted in PDLIM2 and PTEN

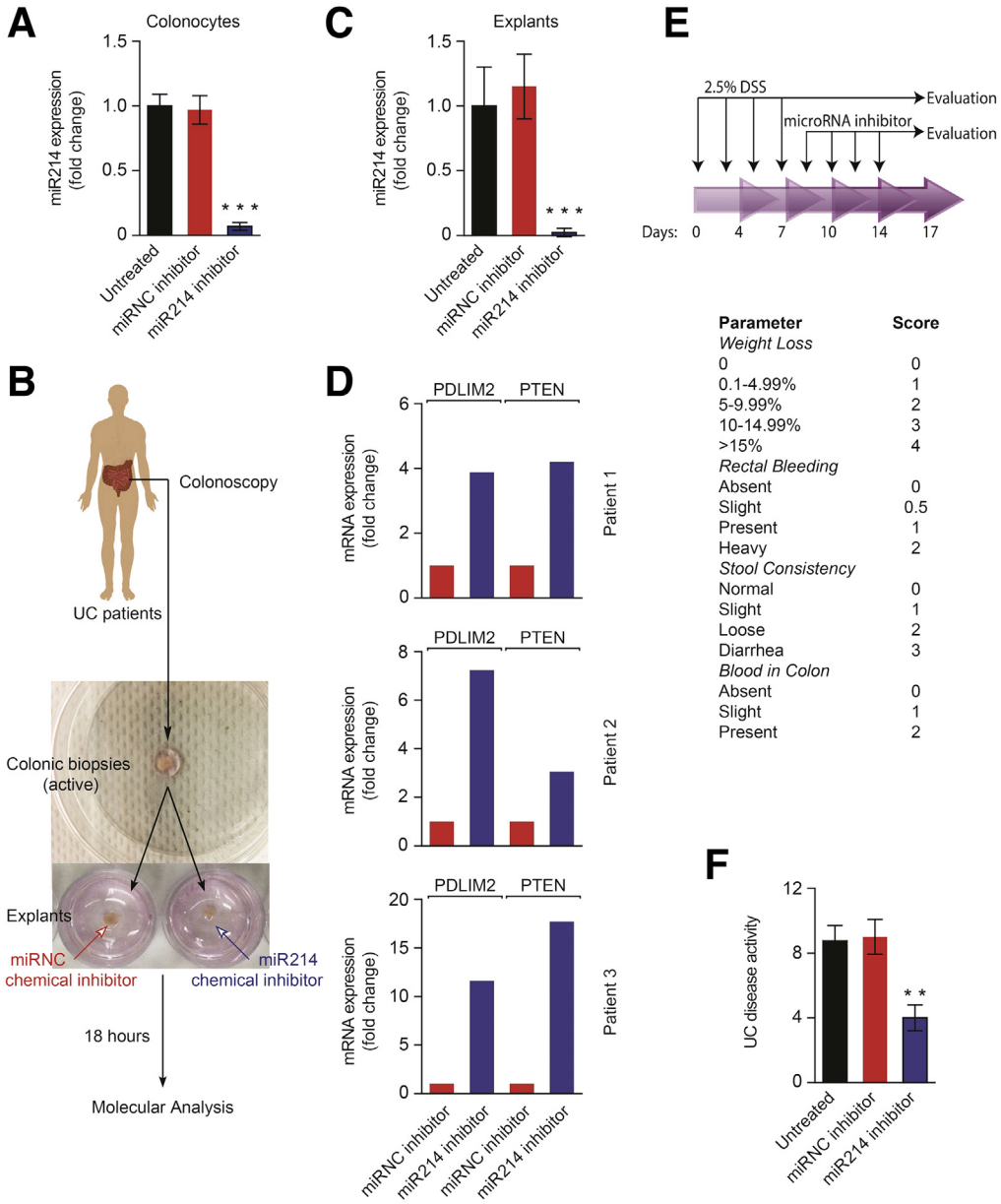

Parameter	Score
Weight Loss	
0	0
0.1-4.99%	1
5-9.99%	2
10-14.99%	3
>15%	4
Rectal Bleeding	
Absent	0
Slight	0.5
Present	1
Heavy	2
Stool Consistency	
Normal	0
Slight	1
Loose	2
Diarrhea	3
Blood in Colon	
Absent	0
Slight	1
Present	2

Figure 4. A chemical inhibitor reverses the effects of miR-214 on colonic tissues from UC patients and ameliorates disease activity in a mouse colitis model. (*A*) A chemical inhibitor effectively suppresses miR-214 expression in colonocytes in vitro. The effectiveness of a miR-214–specific chemical inhibitor was tested in vitro on NCM356 colonocytes. Cells treated with the miR-214 chemical inhibitor (for 30 minutes) were analyzed 24 hours later for miR-214 levels, as assessed by qPCR. Data are shown as the means ± SE. ***$P < .001$ in comparison with untreated and negative control–treated cells, Student *t* test. (*B*) Fresh colonic biopsy specimens isolated at colonoscopy were divided in 2 and treated with the chemical inhibitor against miR-214 or negative control (NC). (*C*) A chemical inhibitor effectively suppresses miR-214 expression in colonic biopsy specimens ex vivo. After treatments, RNA was extracted from biopsy specimens and analyzed for miR-214 levels by qPCR. Data are shown as the means ± SE. ***$P < .001$ in comparison with untreated and negative control–treated biopsy specimens, Student *t* test. (*D*) A chemical inhibitor reverses miR-214 effects in colonic biopsy specimens ex vivo. Biopsy specimens were analyzed for PDLIM2 and PTEN levels by qPCR. (*E*) The therapeutic protocol applied on the chronic DSS mouse model and the criteria used for assessment of the disease activity score. miR-214 inhibitor or the negative control were administered intracolonically in DSS-treated mice after day 8 for 4 cycles (every 2 days). On day 20, the mice were killed, and colon length was measured. (*F*) A chemical inhibitor of miR-214 ameliorates disease activity in the chronic DSS mouse colitis model. Data are shown as the means ± SE. **$P < .01$ in comparison with untreated and NC-treated DSS mice, 4 mice per group, Student *t* test.

suppression (Supplementary Figure 8), Akt phosphorylation (Supplementary Figure 9), and NF-κB activation (Supplementary Figure 10), indicating that the miR-214 feedback loop circuit is hyperactivated during oncogenesis. MiR-214 overexpression suppressed PTEN and PDLIM2 mRNA levels (Supplementary Figure 11), and in support of the human relevance, PDLIM2 and PTEN levels were decreased significantly in tumors from CAC

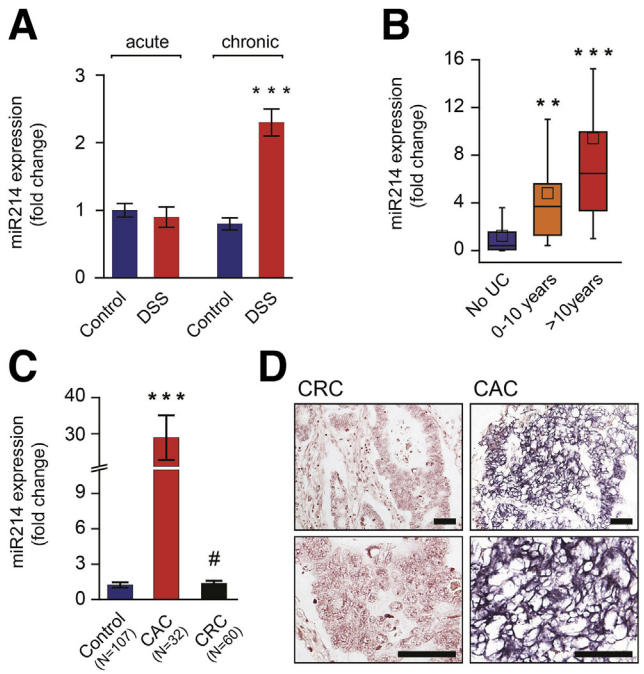

Figure 5. MiR-214 expression correlates with the duration of ulcerative colitis and the development of colitis-associated cancer. (*A*) Chronic colonic inflammation regulates miR-214 expression in mice. Data are shown as the means ± SE. $^{***}P < .001$ in comparison with control (DSS-untreated) mice. (*B*) Chronic colonic inflammation regulates miR-214 expression in UC patients. Data are shown as the means ± SE. $^{**}P < .01$, $^{***}P < .001$ in comparison with control (no UC) tissues. (*C*) miR-214 is hyperexpressed in CAC, but not sporadic CRC, as shown by qPCR. Data are shown as the means ± SE. $^{***}P < .001$ in comparison with control tissues; $^{\#}P < .001$ in comparison with CAC, Student *t* test. (*D*) In situ hybridization indicates the overexpression of miR-214 (blue) in tumors from CAC compared with CRC patients. Nuclear Red was used as counterstain. *Scale bars*: 50 μm.

patients relative to controls (Supplementary Figure 12). In contrast, their levels were not decreased significantly in tumors from CRC patients, supporting the specificity of the miR-214 circuit in CAC (Figure 6*E*). Given that miR-214 increases cancer cell aggressiveness, we examined the miR-214 correlation to colon cancer progression. Examination of human tumors indicated that miR-214 specifically is up-regulated during CAC disease progression (Figure 6*F*), providing additional evidence of the specificity of miR-214 circuit in UC and CAC.

MiR-214 Chemical Inhibitor Suppresses Azoxymethane-DSS–Induced Colon Carcinogenesis

According to our data, the miR-214–positive feedback loop circuit links chronic inflammation to colon carcinogenesis. Therefore, targeting miR-214 may suppress the development of CAC. We applied a therapeutic protocol consisting of intracolonic administration of a chemical miR-214 inhibitor or microRNA-negative control for 4 cycles, weekly (Figure 7*A* and Supplementary Figure 13) on the azoxymethane-DSS mouse model. The miR-214 inhibitor reduced the number (Figure 7*B*) and size (Figure 7*C*) of tumors significantly. Mechanistically, the miR-214 inhibitor suppressed tumor growth through the induction of apoptosis and activation of caspase-3 (Figure 7*D*). In addition, immunohistochemical analysis showed that miR-214 inhibition reduced NF-κB and Akt phosphorylation levels, indicating efficient suppression of the miR-214 molecular circuit, and decreased the proliferation rate of colon cancer cells (Figure 7*E*).

Discussion

MiR-214 expression correlates with UC activity and disease duration and provides the molecular rationale for the current practice guidelines recommending surveillance colonoscopy 8–10 years after diagnosis of UC.[39] Although the association between IBD and cancer, linking colonic inflammation to colorectal cancer risk, was documented as early as 1925,[38] its molecular biology remains unknown. We propose that a microRNA, miR-214, is the central regulator, based on its unique expression pattern in ulcerative colitis–associated colon cancer patients. Our findings suggest that miR-214 could serve as a biomarker identifying patients at risk for this malignant transformation. We also show that miR-214 expression correlates well with disease activity and disease duration, which offers the molecular rationale for the current practice guidelines recommending surveillance colonoscopy for UC patients 8–10 years after diagnosis.[39]

Clinical and epidemiologic studies have shown a strong association between chronic inflammation and the development of cancer through activation of inflammatory molecules.[40,41] IL6 is secreted by epithelial and immune cells contributing to the transformation of normal into malignant cells.[24,28,42] Although inflammatory responses have been found to be activated in both sporadic and colitis-associated colon cancers, it is not clear whether these inflammatory signals regulate the same signaling pathways. Our data show miR-214 as an inflammatory effector molecule that is deregulated in colitis-associated colon cancer patients. The STAT3 transcription factor is able to bind to the promoter area of miR-214, and the presence of IL6 leads to IL6-STAT3–dependent miR-214 expression and thus the regulation of both the PDLIM2–NF-κB and the PTEN-Akt pathways. In addition, miR-214 up-regulation induces the NF-κB–IL6 pathway, suggesting the presence of a miR-214 feedback loop circuit. Gain-of-function and loss-of-function assays confirmed the significance of miR-214 in colorectal oncogenesis. Given that IL6-STAT3 signaling is activated while miR-214 expression is not deregulated in other gastrointestinal diseases, such as CD and CRC, we propose that the responsiveness of the *MIR214* gene to inflammatory signals depends on epigenetic cues deregulated on sustained chronic colonic inflammation. Although we identified feedback loop inflammatory circuits in different human

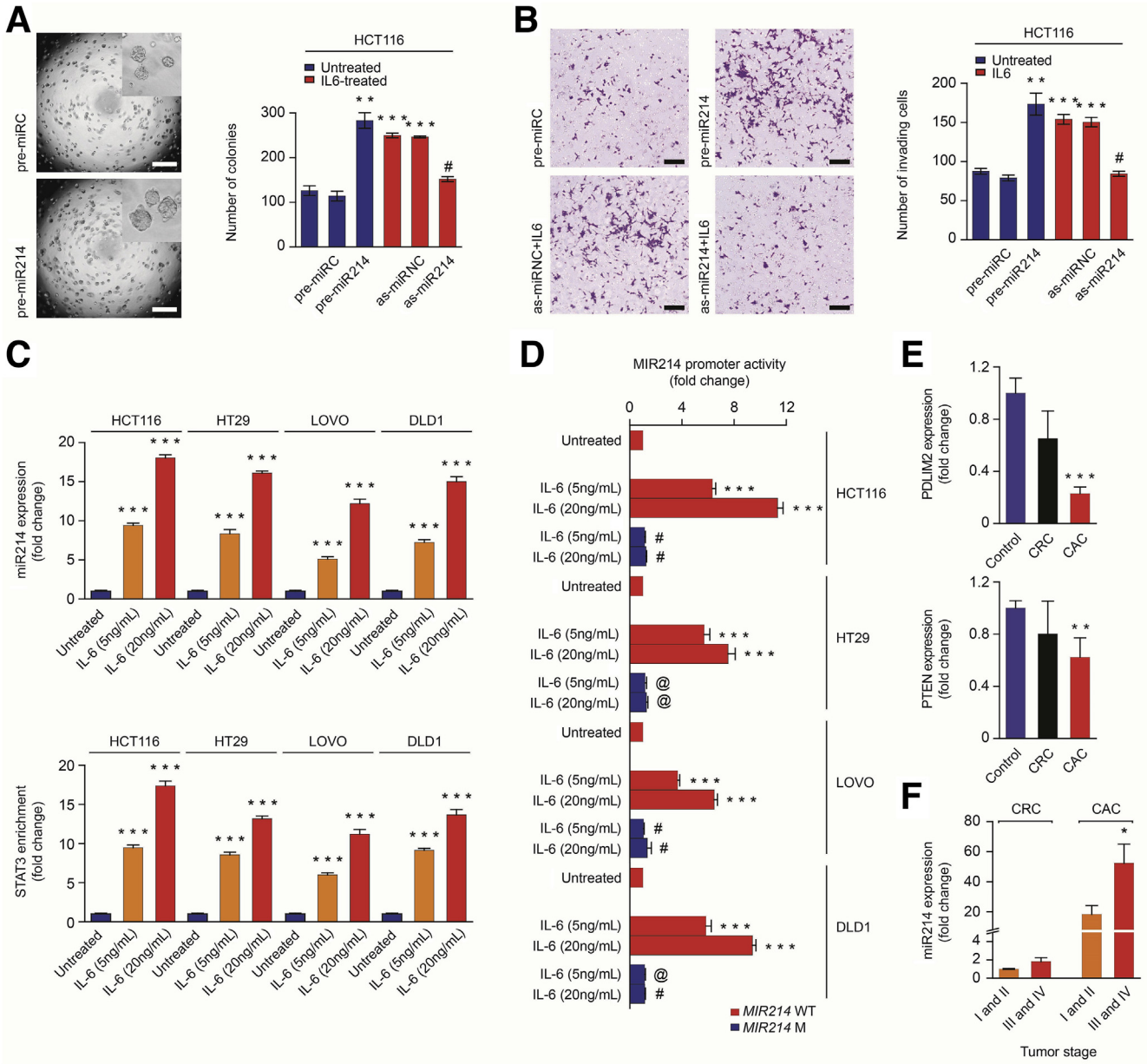

Figure 6. Tumorigenic potential of the miR-214 circuit in human colonocytes. (*A* and *B*) IL6 through miR-214 regulates the tumorigenic properties of colon cancer cells. (*A*) MiR-214 overexpression (pre–miR-214) enhances colon cancer cell colony formation in soft agar, whereas miR-214 inhibition (as–miR-214) reverses the effects of IL6. *Scale bars*: 500 μm. (*B*) MiR-214 overexpression (pre–miR-214) enhances colon cancer cell invasion in Matrigel (BD Biosciences, Franklin Lakes, NJ), whereas miR-214 inhibition (as–miR-214) reverses the effects of IL6. *Scale bars*: 100 μm. Data are shown as the means ± SE. $^{**}P < .01$, $^{***}P < .001$ in comparison with untreated and control (pre–miR-C)-treated cells. $^{\#}P < .001$ in comparison with as–miR-negative control (NC)-treated cells; Student *t* test. (*C*) IL6 dose-dependently induces the expression of miR-214 and the binding of STAT3 on the promoter of the *MIR214* gene, in colon cancer cells. Effects of IL6 on the expression of miR-214, as assessed by qPCR and STAT3 binding, as assessed by chromatin immunoprecipitation and qPCR analysis. Data are shown as the means ± SE. $^{***}P < .001$ in comparison with untreated cells, Student *t* test. (*D*) STAT3 binding on the promoter is required for the transcriptional activation of the *MIR214* gene in colon cancer cells. IL6 induces the luciferase activity of the wild-type (WT) *MIR214* gene promoter, whereas mutagenesis of the STAT3 binding site abolishes promoter activation by IL6. M, mutated STAT3 binding site. Data are shown as the means ± SE. $^{***}P < .001$ in comparison with untreated cells. $^{\#}P < .001$, $^{@}P < .01$ in comparison with the IL6-induced WT promoter activity, Student *t* test. (*E*) PDLIM2 and PTEN expression is suppressed significantly in CAC but not CRC, as assessed by qPCR. Data are shown as the means ± SE. $^{**}P < .01$, $^{***}P < .001$ in comparison with control colonic tissues, Student *t* test. (*F*) MiR-214 levels correlate positively with tumor staging in CAC. Data are shown as the means ± SE. $^{*}P < .05$ in comparison with early CAC stages (I and II), Student *t* test.

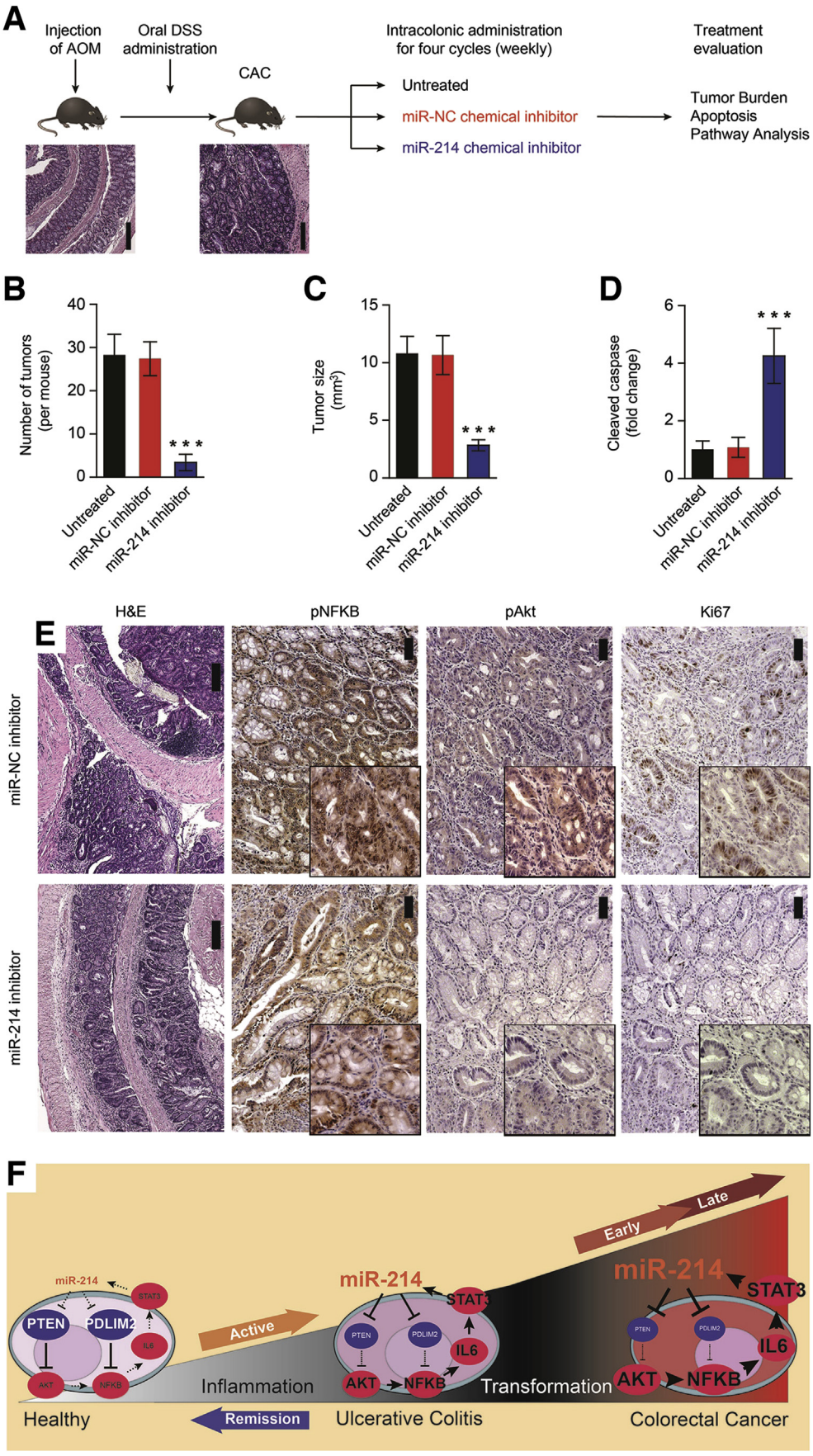

Figure 7. A chemical inhibitor of miR-214 effectively suppresses colitis-associated colorectal cancer in vivo. (*A*) Protocol for anti–miR-214 therapy in the mouse azoxymethane (AOM)-DSS colitis-associated colorectal cancer model. (*B–D*) Evaluation of the therapeutic potential of intracolonic administration of miR-214 inhibitor on the (*B*) number and (*C*) size of tumors, and (*D*) the levels of cleaved caspase 3 in the tumors formed in the AOM-DSS mouse model of colitis-associated colorectal cancer. Data are shown as the means ± SE. ***$P < .001$ in comparison with untreated and control (miR–negative control [NC] inhibitor)-administered mice, 10 mice per group, Student *t* test. (*E*) H&E, pNF-κB (S536), pAkt (S473), and Ki-67 staining in sections of colonic tissues from mice treated with the chemical miR-214 inhibitor or negative control. *Scale bars*: 200 μm (for H&E staining) and 50 μm (for immunohistochemistry). (*F*) Schematic representation of the activity and role of the miR-214 molecular circuit in UC and CAC. In healthy noninflamed colonic epithelial cells, PDLIM2 and PTEN expression suppresses the activation of Akt and NF-κB. During the development of UC, miR-214 targets PDLIM2 and PTEN to activate Akt and NF-κB. In turn, NF-κB regulates IL6 expression and thus STAT3 activity. STAT3-mediated transcriptional activation of miR-214 creates a positive feedback loop circuit that is attenuated when disease is in an inactive state. In long-standing UC, overexpression of miR-214 and hyperactivation of this inflammatory circuit promotes the development of colorectal cancer.

diseases,[24,28] we show a feedback loop mechanism that is involved not only in 2 human diseases (ulcerative colitis and colon cancer), but, importantly, acts as a rheostat, being hyperactivated and contributing to the progression from colitis to colon cancer (Figure 7*F*).

Therapeutic applications are conceivable as shown in our experiments by using the novel miR-214 chemical inhibitor. Studies have shown these microRNA mimics or microRNA inhibitors have a therapeutic potential in different types of cancer and autoimmune diseases. With the recent demonstration that inhibition of miR-122 reduces viral load in HCV-infected chimpanzees,[43] miR-122 inhibitors are already in phase II trials. We recently showed that intravenous administration of a microRNA mimic could have therapeutic potential in liver cancer patients through suppression of the inflammatory response.[24] Here, we showed that intracolonic administration of chemically modified antisense–miR-214 suppresses the development of tumor growth effectively in an animal model of colitis-associated colon cancer, suggesting that a similar approach could be considered for colitis-associated dysplasia and cancer.

Supplementary Material

Note: To access the supplementary material accompanying this article, visit the online version of *Gastroenterology* at www.gastrojournal.org, and at http://dx.doi.org/10.1053/j.gastro.2015.05.057.

References

1. Danese S, Fiocchi C. Ulcerative colitis. N Engl J Med 2011;365:1713–1725.
2. Ananthakrishnan AN, Khalili H, Konijeti GG, et al. Long-term intake of dietary fat and risk of ulcerative colitis and Crohn's disease. Gut 2014;63:776–784.
3. Eaden JA, Abrams KR, Mayberry JF. The risk of colorectal cancer in ulcerative colitis: a meta-analysis. Gut 2001;48:526–535.
4. Ekbom A, Helmick C, Zack M, et al. Ulcerative colitis and colorectal cancer. A population-based study. N Engl J Med 1990;323:1228–1233.
5. Soderlund S, Brandt L, Lapidus A, et al. Decreasing time-trends of colorectal cancer in a large cohort of patients with inflammatory bowel disease. Gastroenterology 2009;136:1561–1567; quiz 1818–1819.
6. Bernstein CN, Blanchard JF, Kliewer E, et al. Cancer risk in patients with inflammatory bowel disease: a population-based study. Cancer 2001;91:854–862.
7. Jess T, Loftus EV Jr, Velayos FS, et al. Risk of intestinal cancer in inflammatory bowel disease: a population-based study from Olmsted County, Minnesota. Gastroenterology 2006;130:1039–1046.
8. Lakatos L, Mester G, Erdelyi Z, et al. Risk factors for ulcerative colitis-associated colorectal cancer in a Hungarian cohort of patients with ulcerative colitis: results of a population-based study. Inflamm Bowel Dis 2006;12:205–211.
9. Palli D, Trallori G, Bagnoli S, et al. Hodgkin's disease risk is increased in patients with ulcerative colitis. Gastroenterology 2000;119:647–653.
10. Farraye FA, Odze RD, Eaden J, et al. AGA medical position statement on the diagnosis and management of colorectal neoplasia in inflammatory bowel disease. Gastroenterology 2010;138:738–745.
11. Delco F, Sonnenberg A. A decision analysis of surveillance for colorectal cancer in ulcerative colitis. Gut 2000;46:500–506.
12. Lindberg JO, Stenling RB, Rutegard JN. DNA aneuploidy as a marker of premalignancy in surveillance of patients with ulcerative colitis. Br J Surg 1999;86:947–950.
13. Lashner BA, Shapiro BD, Husain A, et al. Evaluation of the usefulness of testing for p53 mutations in colorectal cancer surveillance for ulcerative colitis. Am J Gastroenterol 1999;94:456–462.
14. Suzuki H, Harpaz N, Tarmin L, et al. Microsatellite instability in ulcerative colitis-associated colorectal dysplasias and cancers. Cancer Res 1994;54:4841–4844.
15. Karlen P, Young E, Brostrom O, et al. Sialyl-Tn antigen as a marker of colon cancer risk in ulcerative colitis: relation to dysplasia and DNA aneuploidy. Gastroenterology 1998;115:1395–1404.
16. McGovern DP, Gardet A, Torkvist L, et al. Genome-wide association identifies multiple ulcerative colitis susceptibility loci. Nat Genet 2010;42:332–337.
17. **Jostins L, Ripke S**, Weersma RK, et al. Host-microbe interactions have shaped the genetic architecture of inflammatory bowel disease. Nature 2012;491:119–124.
18. Brant SR. Promises, delivery, and challenges of inflammatory bowel disease risk gene discovery. Clin Gastroenterol Hepatol 2013;11:22–26.
19. **Polytarchou C, Koukos G**, Iliopoulos D. Systems biology in inflammatory bowel diseases: ready for prime time. Curr Opin Gastroenterol 2014;30:339–346.
20. Guo H, Ingolia NT, Weissman JS, et al. Mammalian microRNAs predominantly act to decrease target mRNA levels. Nature 2010;466:835–840.
21. Boldin MP, Baltimore D. MicroRNAs, new effectors and regulators of NF-kappaB. Immunol Rev 2012;246:205–220.
22. **Androulidaki A, Iliopoulos D**, Arranz A, et al. The kinase Akt1 controls macrophage response to lipopolysaccharide by regulating microRNAs. Immunity 2009;31:220–231.
23. Stagakis E, Bertsias G, Verginis P, et al. Identification of novel microRNA signatures linked to human lupus disease activity and pathogenesis: miR-21 regulates aberrant T cell responses through regulation of PDCD4 expression. Ann Rheum Dis 2011;70:1496–1506.
24. Hatziapostolou M, Polytarchou C, Aggelidou E, et al. An HNF4alpha-miRNA inflammatory feedback circuit regulates hepatocellular oncogenesis. Cell 2011;147:1233–1247.
25. Baltimore D, Boldin MP, O'Connell RM, et al. MicroRNAs: new regulators of immune cell development and function. Nat Immunol 2008;9:839–845.
26. Wu F, Zikusoka M, Trindade A, et al. MicroRNAs are differentially expressed in ulcerative colitis and alter expression of macrophage inflammatory peptide-2 alpha. Gastroenterology 2008;135:1624–1635 e24.

27. Koukos G, Polytarchou C, Kaplan JL, et al. MicroRNA-124 regulates STAT3 expression and is down-regulated in colon tissues of pediatric patients with ulcerative colitis. Gastroenterology 2013;145:842–852 e2.
28. Iliopoulos D, Hirsch HA, Struhl K. An epigenetic switch involving NF-kappaB, Lin28, Let-7 MicroRNA, and IL6 links inflammation to cell transformation. Cell 2009;139:693–706.
29. **Hatziapostolou M, Polytarchou C**, Iliopoulos D. miRNAs link metabolic reprogramming to oncogenesis. Trends Endocrinol Metab 2013;24:361–373.
30. Iliopoulos D, Jaeger SA, Hirsch HA, et al. STAT3 activation of miR-21 and miR-181b-1 via PTEN and CYLD are part of the epigenetic switch linking inflammation to cancer. Mol Cell 2010;39:493–506.
31. Pekow JR, Kwon JH. MicroRNAs in inflammatory bowel disease. Inflamm Bowel Dis 2012;18:187–193.
32. Tanaka T, Grusby MJ, Kaisho T. PDLIM2-mediated termination of transcription factor NF-kappaB activation by intranuclear sequestration and degradation of the p65 subunit. Nat Immunol 2007;8:584–591.
33. Polytarchou C, Iliopoulos D, Hatziapostolou M, et al. Akt2 regulates all Akt isoforms and promotes resistance to hypoxia through induction of miR-21 upon oxygen deprivation. Cancer Res 2011;71:4720–4731.
34. Romashkova JA, Makarov SS. NF-kappaB is a target of AKT in anti-apoptotic PDGF signalling. Nature 1999;401:86–90.
35. Dan HC, Cooper MJ, Cogswell PC, et al. Akt-dependent regulation of NF-{kappa}B is controlled by mTOR and Raptor in association with IKK. Genes Dev 2008;22:1490–1500.
36. Im E, Jung J, Pothoulakis C, et al. Disruption of Pten speeds onset and increases severity of spontaneous colitis in Il10 mice. Gastroenterology 2014;147:667–679.e10.
37. **Warner JB, Philippakis AA, Jaeger SA**, et al. Systematic identification of mammalian regulatory motifs' target genes and functions. Nat Methods 2008;5:347–353.
38. Crohn UB, Rosenberg H. The sigmoidoscopic picture of chronic ulcerative colitis (non-specific). Am J Med Sci 1925;170:220–228.
39. Farraye FA, Odze RD, Eaden J, et al. AGA technical review on the diagnosis and management of colorectal neoplasia in inflammatory bowel disease. Gastroenterology 2010;138:746–774. 774 e1–4; quiz e12–e13.
40. Balkwill F, Mantovani A. Inflammation and cancer: back to Virchow? Lancet 2001;357:539–545.
41. Naugler WE, Karin M. NF-kappaB and cancer-identifying targets and mechanisms. Curr Opin Genet Dev 2008;18:19–26.
42. He G, Karin M. NF-kappaB and STAT3–key players in liver inflammation and cancer. Cell Res 2011;21:159–168.
43. **Lanford RE, Hildebrandt-Eriksen ES, Petri A**, et al. Therapeutic silencing of microRNA-122 in primates with chronic hepatitis C virus infection. Science 2010;327:198–201.

Author names in bold designate shared co-first authors.

Received January 7, 2015. Accepted May 30, 2015.

Reprint requests
Address requests for reprints to: Dimitrios Iliopoulos, PhD, MBA, Center for Systems Biomedicine, Division of Digestive Diseases, David Geffen School of Medicine, University of California at Los Angeles, 650 Charles E. Young Drive, CHS 44-133, Los Angeles, California 90095-7278. e-mail: diliopoulos@mednet.ucla.edu; fax: (310) 825–8857.

Conflicts of interest
The authors disclose no conflicts.

Funding
Supported in part by the National Center for Advancing Translational Sciences University of California at Los Angeles Clinical and Translational Science Institute grant UL1TR000124 and the Broad Medical Research Program at Crohn's & Colitis Foundation of America (C.P.), a Cancer Research Institute Investigator Award (D.I.), The Leona M. and Harry B. Helmsley Charitable Trust (D.I.), and National Institutes of Health National Institute of Diabetes and Digestive and Kidney Diseases grant RO1 DK60729 (C.P.).

Supplementary Materials and Methods

Materials

Human colon cancer cell lines (American Type Culture Collection, Manassas, VA) were cultured under standard culture conditions, and NCM356 and NCM460 were grown in M3:10 (INCELL, San Antonio, TX). IL6 (200-06; Peprotech, Rocky Hill, NJ) was used to stimulate cells, whereas MK2206 (S1078) and BAY 11-7082 (S2913; Selleckchem, Houston, TX) were used to inhibit Akt and NF-κB, respectively. Antibodies used in Western blot analyses were phospho–NF-κB p65 (Ser536) (3033), phospho-STAT3 (Tyr705) (9145), NF-κB p65 (8242), STAT3 (9139), PDLIM2 (8144), PTEN (9188; Cell Signaling Technology), and α-tubulin (T5168; Sigma, St. Louis, MO).

Bioinformatic Analysis

The Lever and PhylCRM algorithms have been used to identify STAT3 binding motifs in an area 5 kb upstream and 2 kb downstream of microRNAs.

In Situ Hybridization

Double-digoxigenin–labeled miRCURY Locked Nucleic Acid Detection probe for the detection of miR-214 (38494-15; Exiqon) by in situ hybridization was used as previously described with modifications(*13*). Sections of control, ulcerative colitis, and colorectal carcinomas were deparaffinized with xylene (3 times for 5 minutes), followed by treatment with serial dilutions of ethanol (3 times in 100%, twice in 96%, and 3 times in 70%), and by 2 changes of Diethyl pyrocarbonate–phosphate-buffered saline. Tissues then were digested with proteinase K (15 mg/mL) for 30 minutes at 37°C and rinsed 3 times with Diethyl pyrocarbonate–phosphate-buffered saline. Sections were dehydrated twice with 70%, 96%, and 100% ethanol, air-dried, and hybridized for 1 hour with the homo sapiens-miR-214 (40 nmol/L) diluted in microRNA in situ hybridizatin buffer (90000; Exiqon, Woburn, MA) at 60°C. After hybridization, sections were rinsed twice with 5× standard saline citrate, twice with 1× standard saline citrate, and 3 times with 0.2× standard saline citrate, for 5 minutes each, at 60°C, and phosphate-buffered saline. The slides were incubated with blocking solution (11585762001; Sigma-Aldrich, Saint Louis, MO) for 15 minutes and then with anti-digoxigenin antibody (1:800) in 2% sheep serum (013-000-121; Jackson Immunoresearch, West Grove, PA) blocking solution for 1 hour, at room temperature. After 3 washes with phosphate-buffered saline, 0.1% Tween-20, slides were incubated with the AP substrate buffer (nitro blue tetrazolium - 5-bromo-4-chloro-3-indolyl-phosphate tablet [11697471001, Roche] in 10 mL 0.2 mmol/L Levamisole [31742; Sigma-Aldrich]) for 2 hours at 30°C in the dark. The reaction was stopped with 2 washes of AP stop solution (50 mmol/L Tris-HCl, 150 mmol/L NaCl, and 10 mmol/L KCl) and 2 washes with water. Tissues were counterstained with Nuclear Fast Red (Sigma-Aldrich) for 1 minute and rinsed with water. At the end, sections were dehydrated twice with 70%, 96%, and 100% ethanol and mounted with coverslips in Eukitt mounting medium (361894G; VWR, Visalia, CA). Images were captured with a Nikon 80i upright microscope equipped with a Nikon Digital Sight DS-Fi1 (Nikon, Melville, NY) color camera, using the NIS-Elements image acquisition software (Nikon). All images were captured and processed using identical settings.

Immunohistochemistry

For tissue immunostaining for phospho–NF-κB, phospho-Akt, and Ki67, formalin fixed paraffin embedded sections of colonic tissues from azoxymethane-DSS mice treated with the chemical miR-214 inhibitor or negative control were deparaffinized with xylene (3 × 5 minutes) followed by treatment with serial dilutions of ethanol (100%, 100%, 95%, and 95%, 10 minutes each) and by 2 changes of ddH_2O. Antigen unmasking was achieved by boiling the slides (95°C–99°C) for 10 minutes, in 10 mmol/L sodium citrate, at pH 6.0. Sections were rinsed 3 times with ddH_2O, immersed in 3% H_2O_2 for 20 minutes, washed twice with distilled deionized water and once with Tris-buffered saline and 0.1% Tween-20, and blocked for 1 hour with blocking solution (5% normal goat serum [5425; Cell Signaling Technology, Danvers, MA] in Tris-buffered saline and 0.1% Tween-20). Phospho-P65 (Ser536) (SAB4300009; Sigma-Aldrich), phospho-Akt (Ser473) (4060; Cell Signaling Technology), and Ki67 (12202; Cell Signaling Technology) antibodies were diluted 1:200, 1:50, and 1:400, respectively, in Signal Stain antibody diluent (8112; Cell Signaling Technology) and incubated with the sections overnight at 4°C. After incubation with the antibodies, sections were washed 3 times, for 5 minutes each, with Tris-buffered saline and 0.1% Tween-20 and incubated for 1 hour at room temperature with Signal Stain Boost (horseradish peroxidase, rabbit [8114], or horseradish peroxidase, mouse [8125]; Cell Signaling Technology). Sections were washed 3 times, for 5 minutes each, with Tris-buffered saline and 0.1% Tween-20, and stained with the 3,3′-diaminobenzidine tetra hydrochloride Peroxidase Substrate Kit (SK-4100; Vector Laboratories, Burlingame, CA) for 30 minutes, washed, and counterstained with the hematoxylin QS (H-3404; Vector Laboratories). Finally, tissues were dehydrated and mounted in Eukitt medium. Microscope equipped with a Nikon Digital Sight DS-Fi1 color camera, using the NIS-Elements image acquisition software. All images were captured and processed using identical settings.

Quantitative Real-Time PCR Analysis

Real-time PCR was performed to determine the expression levels of miR-214 in human colon carcinomas and tissues. RNA was isolated, using TRIzol (15596-026; Invitrogen, Carlsbad, CA). Reverse transcription was performed using the Universal complementary DNA synthesis kit (203300; Invitrogen). Real-time PCR was performed in triplicate using the SYBR Green master mix (203450) and primers for miR-214 (204510; Exiqon) in a CFX384 Real Time PCR detection system (Bio-Rad, Hercules, CA). *MIR214* expression levels were normalized to the levels of U6 small nuclear RNA (203907; Exiqon).

Real-time PCR was used to determine the expression levels of *PTEN* and *PDLIM2*. Reverse transcription was performed using the Retroscript Kit (AM1710; Applied Biosystems, Foster City, CA). Real-time PCR was performed using the IQ SYBR Green supermix (170-8882; Bio-Rad). *Glyceraldehyde-3-phosphate dehydrogenase* and *B-actin* were used as the internal control. The sequences of the primers used were as follows: *PTEN*-F: 5'-cccagacatgacagccatc-3'; *PTEN*-R: 5'-tctgcaggaaatcccatagc-3'; *PDLIM2*-F: 5'-atggccacgattatgtctcc-3'; *PDLIM2*-R: 5'-gcccatcatggtgactaagg-3'; *B-actin*-F: 5'-cccagcacaatgaagatcaa-3'; *B-actin*-R: 5'-acatctgctggaaggtggac-3'*; glyceraldehyde-3-phosphate dehydrogenase*-F: 5'-atgttcgtcatgggtgtgaa-3'; *glyceraldehyde-3-phosphate dehydrogenase*-R: 5'-ggtgctaagcagttggtggt-3'.

Animal Studies

Mouse studies were approved by the University of California Institutional Animal Care and Use Committee and conformed to the US National Institutes of Health Guide for the Care and Use of Laboratory Animals. The therapeutic potential of the miR-214 inhibition was tested in a mouse model of CAC. CAC is induced by administration of 12.5 mg/kg azoxymethane at day 1 followed by repeated oral administration of 3% DSS on days 8, 29, and 50. According to our treatment protocol, locked nucleic acid miR-NC or locked nucleic acid miR-214 inhibitor were administered intracolonically in azoxymethane-DSS–treated mice on a weekly basis for 4 cycles (days 64, 70, 77, and 84).

For the inhibition of miR-214 expression, a locked nucleic acid targeting the miR-214 sequence (5'-TGTCTG TGCCTGCTG-3') was used. The locked nucleic acid, often referred to as *inaccessible RNA*, consists of modified RNA nucleotides. The ribose moiety of a locked nucleic acid nucleotide is modified with an extra bridge connecting the 2' oxygen and 4' carbon. The locked ribose conformation enhances base stacking and backbone pre-organization. This modification significantly increases the specificity and hybridization properties with the target sequence (miR-214). These oligonucleotides also are phosphorothioate-modified. Phosphorothioate modifications provide protection against RNase activity and their lipophilicity contributes to enhanced tissue uptake. For intracolonic administration animals were lightly anesthetized and a polyethylene cannula (Intramedic PE-20 tubing; Becton Dickinson, Parsippany, NJ) was inserted into the colon via the anus. The locked nucleic acid miR-214 inhibitor was diluted in phosphate-buffered saline (2.5 mg/mL) and instilled into the colons using a syringe at a dose of 12 mg/kg, whereas control animals were treated with locked nucleic acid miR-NC (Exiqon, Danvers, MA). On day 91, the mice were killed and the tumor burden was assessed.

Ex Vivo Biopsy Treatment

Fresh human colonic biopsy specimens from patients with active disease, obtained by colonoscopy, were transported immediately to the laboratory in RPMI-1640 medium on ice. Biopsy specimens were divided in 2 and placed in organ culture dishes (48 wells) with RPMI-1640 medium containing 10% fetal calf serum. Colonic explant cultures were treated with locked nucleic acid miR-214 inhibitor or locked nucleic acid miR-NC (25 μg/mL) for 18 hours at 37°C with 95% O_2 and 5% CO_2. After culture for 18 hours, tissue homogenates were subjected to RNA isolation. RNAs were used for qPCR.

BioPlex Enzyme-Linked Immunosorbent Assays

We used a sandwich enzyme-linked immunosorbent assay to assess the phosphorylation status of tyrosine 705 of STAT3 protein in control colonic tissues and samples from patients with ulcerative colitis and colitis-associated cancer, the levels of cleaved caspase-3 in colonic tumors derived from azoxymethane-DSS–treated mice, the phosphorylation status of serine 473 of Akt protein, the phosphorylation status of serine 536 of NF-κB protein, and the secretion of IL6 in colonic cell lines. The data were analyzed in a BioPlex FlexMap3D (Bio-Rad) analyzer using the BioPlex Manager software.

Luciferase Assays

Colonic epithelial cells were transfected with a firefly luciferase reporter gene construct containing the promoter of *MIR214*. Cells were treated with IL6 for 24 hours after transfection of the luciferase vector. Cell extracts were prepared 24 hours later, and luciferase activity was measured using the Dual Luciferase Reporter Assay System (Promega, WI). For the 3'UTR assays, cells were transfected with the reporter vectors carrying the 3'UTR of *PTEN* or *PDLIM2*. At 24 hours they were transfected with miR-214 (or miR-scramble), and at 48 hours luciferase activity was measured using the Dual Luciferase Reporter Assay System.

Invasion Assays

We performed invasion assays in colonic epithelial cell lines 24 hours after transfection with miR-214 or anti–miR-214 or their respective controls. Invasion in Matrigel was conducted using standardized conditions with BDBioCoat growth factor reduced Matrigel invasion chambers (PharMingen, Franklin Lakes, NJ). Assays were conducted according to the manufacturer's protocol, using 2% fetal bovine serum as a chemoattractant. Noninvading cells on the top side of the membrane were removed whereas invading cells were fixed and stained with 4'-6-diamidino-2-phenylindole (Vector Laboratories, Inc) 16 hours after seeding. In all assays, 10 fields per insert were scored and the SE was calculated.

Colony Formation Assays

Colonic epithelial cells were transfected with miR-214 or anti–miR-214 or their respective controls. Then, triplicate samples of 10^5 cells from each cell line were mixed 4:1 (vol/vol) with 2.0% agarose in growth medium for a final concentration of 0.4% agarose. The cell mixture was plated on top of a solidified layer of 0.8% agarose in growth medium. The number of colonies was counted after 6 days.

Chromatin Immunoprecipitation

Chromatin immunoprecipitation was performed as described previously. Briefly, the chromatin fragments, derived from untreated and IL6-treated colonic epithelial cells, were immunoprecipitated with 6 ug of antibody against STAT3. DNA extraction was performed using the Qiagen Purification Kit (Qiagen, Valencia, CA). Real-time PCR analysis was performed for the STAT3 binding site in the *MIR214* promoter using the following primers: forward: 5'-CAAATTCCCCTCCCCTTTTA-3' and reverse 5'-CAATCCTTGGACAATACTGTGTTT-3' (product size: 111 bp).

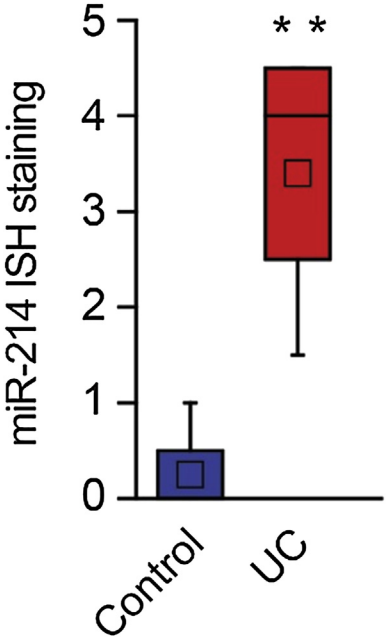

Supplementary Figure 1. miR-214 is up-regulated in the colonic epithelium of human active UC samples. Quantification of miR-214 staining using in situ hybridization. Scoring was performed independently by 2 investigators, blind to the sample IDs. N = 4 per group.

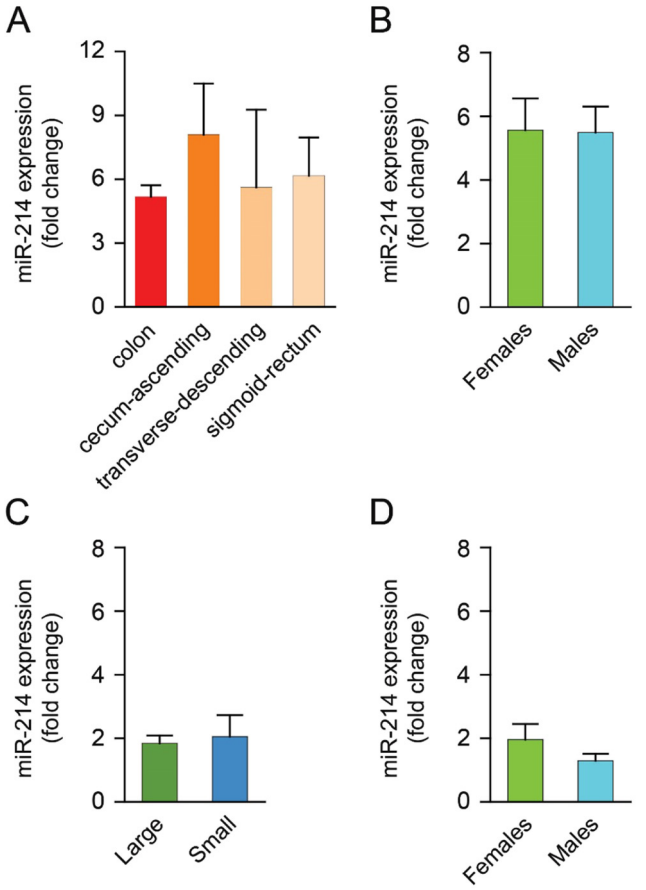

Supplementary Figure 2. miR-214 expression in patients with ulcerative colitis and Crohn's disease. miR-214 expression, as assessed by qPCR, in UC patients does not correlate to the (*A*) anatomic site of the colon or (*B*) sex, and does not differ in CD patients based on (*C*) disease location or (*D*) sex. Data are shown as the means ± SE.

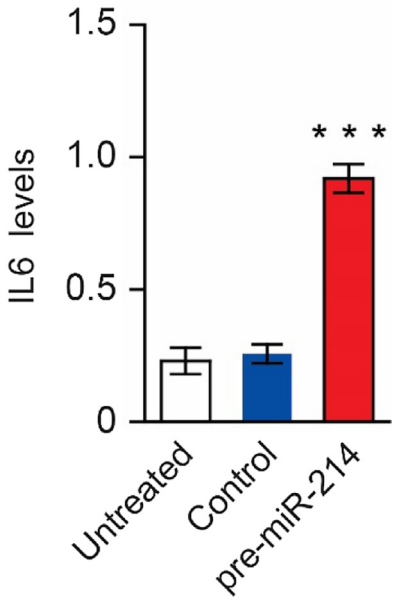

Supplementary Figure 3. miR-214 regulates the expression of IL6 in colonic epithelial cells. Effect of miR-214 on the expression of IL6 in NCM460 cells, as assessed by qPCR. Data are shown as the means ± SE. ***$P < .001$ in comparison with untreated and control (scramble) miR-treated cells, Student *t* test.

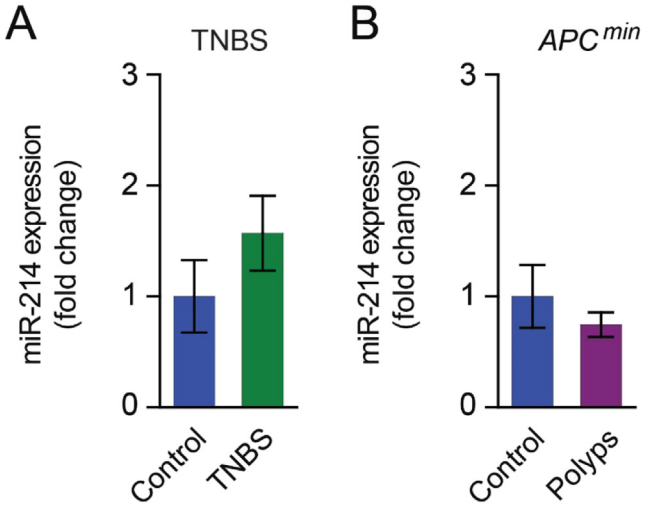

Supplementary Figure 5. miR-214 levels are not deregulated in other inflammation-associated mouse models. (*A*) 2,4,6-trinitrobenzenesulfonic acid (TNBS)-induced colonic inflammation does not deregulate miR-214 expression. Data are shown as the means ± SE, in comparison with control (TNBS-untreated) mice, 4 mice per group. (*B*) Polyp formation in the *APC*^{min} mouse model does not involve changes in the expression of miR-214. Data are shown as the means ± SE, in comparison with control (no polyps) tissues, 5 tissues per group.

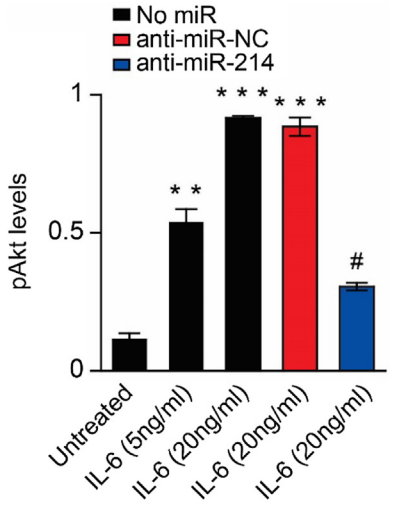

Supplementary Figure 4. IL6 induces Akt phosphorylation in colonocytes through miR-214. Effect of miR-214 inhibition on IL6-induced Akt phosphorylation (S473), as assessed by enzyme-linked immunosorbent assay. Data are shown as the means ± SE. **$P < .01$, ***$P < .001$ in comparison with untreated cells, #$P < .001$ in comparison with negative control (NC) miR-treated cells, Student *t* test.

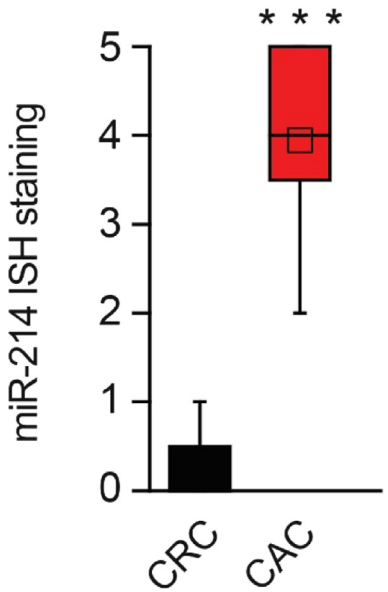

Supplementary Figure 6. miR-214 is up-regulated significantly in colitis-associated colorectal cancer compared with sporadic colorectal cancer. Quantification of miR-214 staining using in situ hybridization. Scoring was performed independently by 2 investigators, blind to the sample IDs. N = 4 for CRC and N = 9 for CAC. ***$P < .001$.

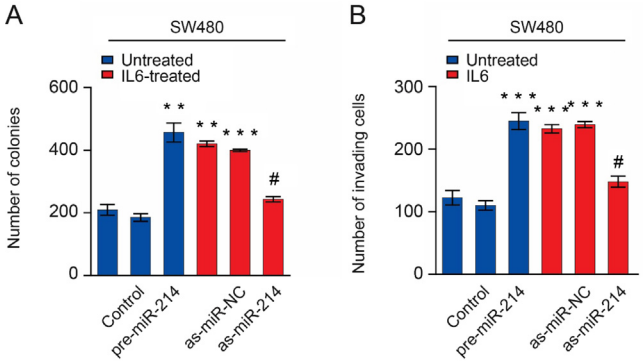

Supplementary Figure 7. miR-214 induces the tumorigenic potential of colon cancer cells and mediates the tumorigenic effects of IL6. miR-214 overexpression enhances the tumorigenic potential, whereas miR-214 inhibition reverses the tumorigenic effects of IL6, on colon cancer cells. Effects of miR-214 overexpression and miR-214 inhibition on IL6-induced (*A*) colony formation in soft agar, and (*B*) invasion of SW480 cells. Data are shown as the means ± SE. $^{**}P < .01$, $^{***}P < .001$ in comparison with untreated cells and control (miR-scramble)-treated cells. $^{\#}P < .001$ in comparison with anti–miR-negative control (NC)-treated cells, Student *t* test.

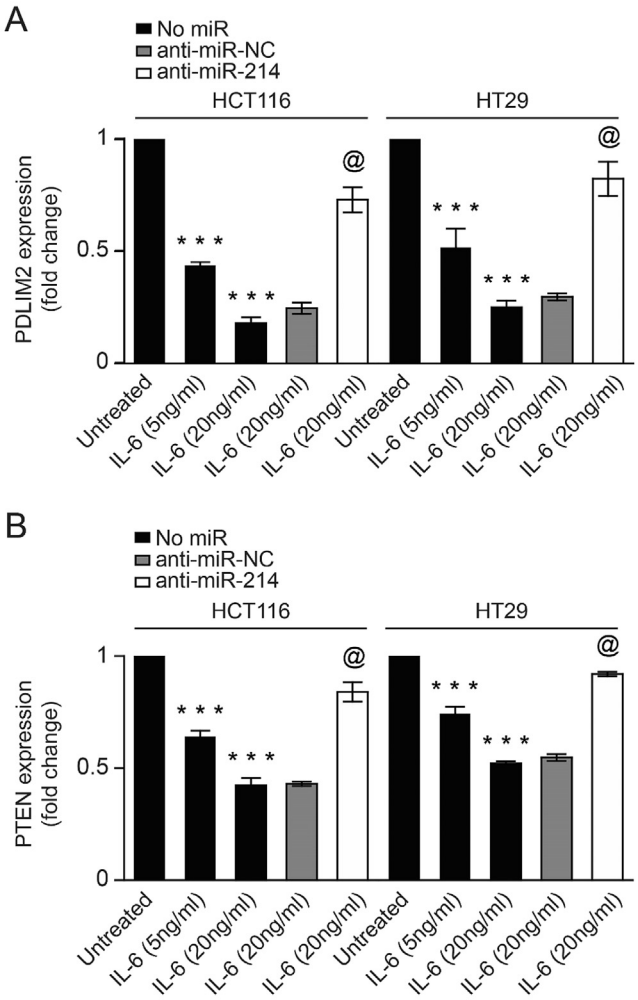

Supplementary Figure 8. IL6 suppresses the expression of PDLIM2 and PTEN in colon cancer cells through miR-214. Effects of IL6 and inhibition of miR-214 on the expression of (*A*) PDLIM2 and (*B*) PTEN mRNA, as assessed by qPCR, in HCT116 and HT29 cells. Data are shown as the means ± SE. $^{***}P < .001$ in comparison with untreated cells; $^{@}P < .01$ in comparison with the anti–miR-negative control (NC)-treated cells, Student *t* test.

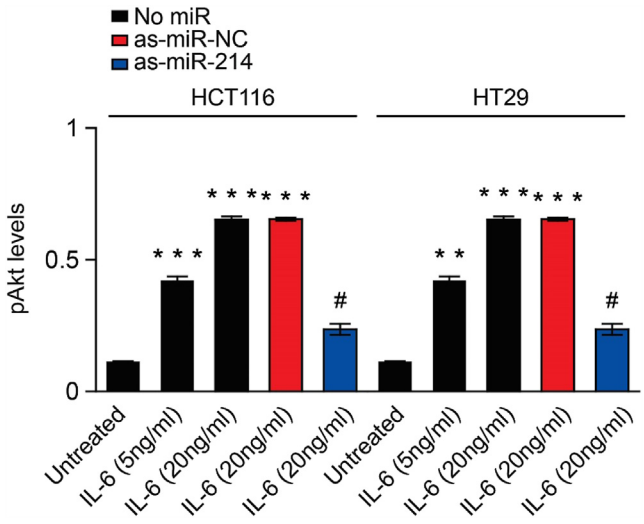

Supplementary Figure 9. IL6 induces the phosphorylation of Akt in colon cancer cells through miR-214. Effect of miR-214 inhibition (as–miR-214) on IL6-induced Akt phosphorylation (S473), as assessed by enzyme-linked immunosorbent assay. Data are shown as the means ± SE. $^{**}P < .01$, $^{***}P < .001$ in comparison with untreated cells; $^{\#}P < .001$ in comparison with control (as–miR-NC)-treated cells, Student *t* test. NC, negative control.

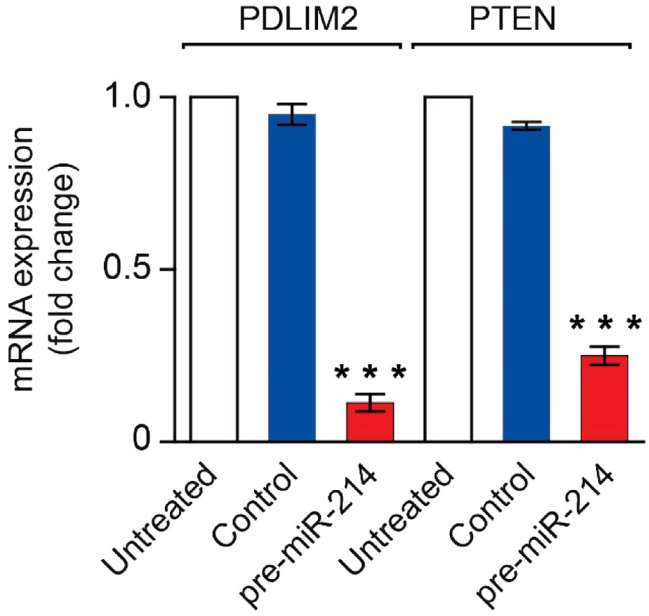

Supplementary Figure 11. MiR-214 regulates the expression of PDLIM2 and PTEN in colon cancer cells. Effects of miR-214 on the levels of PDLIM2 and PTEN mRNA in HCT116 cells, as assessed by qPCR. $^{***}P < .001$ in comparison with untreated and control (pre–miR-C)-treated cells, Student *t* test.

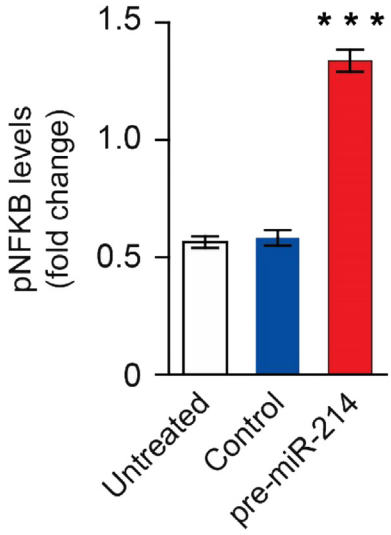

Supplementary Figure 10. MiR-214 regulates the phosphorylation of NF-κB in colon cancer cells. Effects of miR-214 on the levels of pNF-κB (S536) in HCT116 cells, as assessed by enzyme-linked immunosorbent assay. Data are shown as the mean ± SE. $^{***}P < .001$ in comparison with untreated and control (pre–miR-C)-treated cells, Student *t* test.

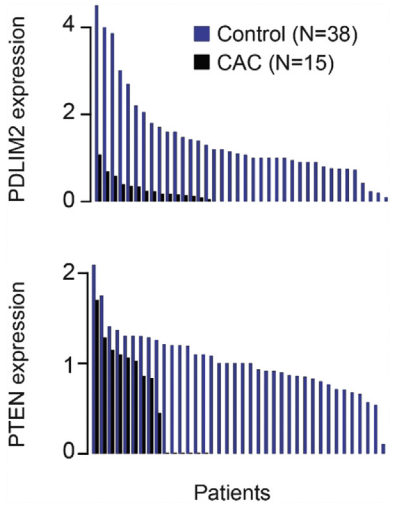

Supplementary Figure 12. PDLIM2 and PTEN expression is down-regulated in colon tumors from CAC patients. PDLIM2 and PTEN mRNA levels in CAC and control colonic tissues was assessed by qPCR.

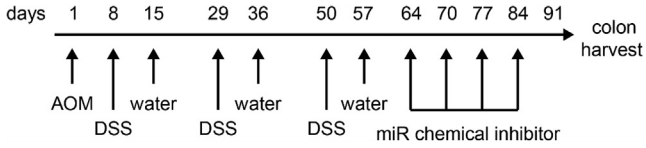

Supplementary Figure 13. The therapeutic protocol applied on the azoxymethane (AOM)-DSS mouse model. To address the therapeutic potential of miR-214 inhibition we used a mouse model of colitis-associated colorectal cancer. In this model colorectal cancer was induced by administration of AOM followed by repeated oral administration of DSS. Chemical microRNA negative control (miR-NC) or miR-214 inhibitor were administered intracolonically in AOM-DSS–treated mice on a weekly basis for 4 cycles. On day 91, the mice were killed and the tumor burden was assessed.

Supplementary Table 1. Cohorts of Patients Analyzed for miR-214 Expression

Cohorts	Control	UC	CD	IBS	CAC	CRC
UCLA	43	18	24	22	6	18
Leiden	52	63	13		22	27
Origene	12	39	23		4	15
Total patients	107	120	60	22	32	60

IBS, irritable bowel syndrome; UCLA, University of California at Los Angeles.

Supplementary Table 2. Characteristics of Patients Analyzed for miR-214 Expression

Groups	Control	UC	CD	IBS	CAC	CRC
Patients, n	107	120	60	22	32	60
Age, *y*						
Median	42	39.5	33	38.5	55.5	70
Range	16–80	20–72	17–74	18–55	25–82	31–91
Missing data	9	10				
P value		NS	NS	NS	[a]	[a,b]
Sex, n (%)						
Female	31 (29)	41 (34)	15 (25)	11 (50)	18 (56)	28 (47)
Male	57 (53)	44 (37)	29 (48)	11 (50)	14 (44)	32 (53)
Missing data	19 (18)	35 (29)	16 (27)			
P value		NS	NS	NS	NS	NS (0.192)
Disease duration		11 (0.3–30)				
TNM stage, n (%)						
I					6 (19)	13 (22)
II					16 (50)	19 (32)
III					7 (22)	18 (30)
IV					3 (9)	10 (17)
P value						NS (0.390)

IBS, irritable bowel syndrome.
[a] $P < .001$ between groups (Kruskall–Wallis test).
[b] $P < .001$ in comparison with CAC (Wilcoxon 2-sample test).

Supplementary Table 3. Expression of miR-214 Targets vs Control (miR-Scramble) in Colonic Epithelial Cells

Symbol	ID	Name	Fold change	*P*
ABR	29	Active BCR-related	−2.16	[a]
ACER3	55331	Alkaline ceramidase 3	−1.67	[a]
ADSS	159	Adenylosuccinate synthase	−3.57	[a]
AP3B1	8546	Adaptor-related protein complex 3, β 1 subunit	−1.53	[b]
ARPC5L	81873	Actin-related protein 2/3 complex, subunit 5-like	−2.07	[a]
BAZ2A	11176	Bromodomain adjacent to zinc finger domain, 2A	−1.79	[a]
BRPF3	27154	Bromodomain and PHD finger containing, 3	−1.58	[a]
CD151	977	CD151 molecule (Raph blood group)	−2.62	[a]
CDC25B	994	Cell division cycle 25 homolog B (*S pombe*)	−1.90	[a]
CDIPT	10423	CDP-diacylglycerol–inositol 3-phosphatidyltransferase	−1.79	[a]
CEP85	64793	Centrosomal protein 85 kilodaltons	−1.57	[a]
CHMP4B	128866	Charged multivesicular body protein 4B	−1.69	[a]
CPEB4	80315	Cytoplasmic polyadenylation element binding protein 4	−1.92	[a]
CTDSP1	58190	CTD (carboxy-terminal domain, RNA polymerase II, polypeptide A) small phosphatase 1	−1.70	[a]
CTSS	1520	Cathepsin S	−2.12	[a]
DNAJC5	80331	DnaJ (Hsp40) homolog, subfamily C, member 5	−1.59	[a]
F8	2157	Coagulation factor VIII, procoagulant component	−1.62	[a]
FAM134A	79137	Family with sequence similarity 134, member A	−3.66	[a]
FAM189B	10712	Family with sequence similarity 189, member B	−1.99	[a]
GALNT7	51809	UDP-N-acetyl-α-D-galactosamine:polypeptide N-acetylgalactosaminyltransferase 7	−2.08	[a]
GLI3	2737	GLI family zinc finger 3	−2.13	[a]
HMG20A	10363	High-mobility group 20A	−1.75	[a]
IGSF3	3321	Immunoglobulin superfamily, member 3	−1.64	[a]
INO80C	125476	INO80 complex subunit C	−2.40	[a]
INTS2	57508	Integrator complex subunit 2	−1.61	[a]
IPO11	51194	Importin 11	−2.06	[a]
ITCH	83737	Itchy E3 ubiquitin protein ligase	−1.67	[a]
KLHDC3	116138	Kelch domain containing 3	−1.56	[a]
KLK10	5655	Kallikrein-related peptidase 10	−1.71	[a]
LAPTM4B	55353	Lysosomal protein transmembrane 4β	−1.84	[a]
LARP1	23367	La ribonucleoprotein domain family, member 1	−2.12	[a]
LEPROTL1	23484	Leptin receptor overlapping transcript-like 1	−2.24	[a]
MED19	219541	Mediator complex subunit 19	−1.90	[a]
MTM1	4534	Myotubularin 1	−1.56	[a]
NAA15	80155	N(α)-acetyltransferase 15, NatA auxiliary subunit	−2.94	[a]
OTUB1	55611	OTU domain, ubiquitin aldehyde binding 1	−1.59	[a]
PAPD5	64282	PAP-associated domain containing 5	−1.73	[a]
PDLIM2	64236	PDZ and LIM domain 2 (mystique)	−3.37	[a]
PGGT1B	5229	PGGT1B	2.25	[a]
PLA2G15	23659	Phospholipase A2, group XV	−1.66	[a]
PLK4	10733	Polo-like kinase 4	−1.55	[a]
POLE3	54107	Polo-like kinase 4	−1.55	[a]
PPP2CB	5516	Protein phosphatase 2, catalytic subunit, β isozyme	−1.68	[a]
PPP6C	5537	Protein phosphatase 6, catalytic subunit	−1.72	[a]
PSMD10	5716	Proteasome (prosome, macropain) 26S subunit, non–adenosine triphosphatase, 10	−3.19	[a]
PTEN	5728	Phosphatase and tensin homolog	−2.47	[a]
RAB14	51552	RAB14, member RAS oncogene family	−2.54	[a]
RASSF5	83593	Ras association (RalGDS/AF-6) domain family member 5	−1.52	[a]
RBM22	55696	RNA binding motif protein 22	−2.46	[a]
RNF115	27246	Ring finger protein 115	−1.71	[a]
RPIA	22934	Ribose 5-phosphate isomerase A	−1.57	[a]
SEC24C	9632	SEC24 family, member C (*S cerevisiae*)	−1.95	[a]
SLC25A44	9673	Solute carrier family 25, member 44	−2.02	[a]
SLC7A8	23428	Solute carrier family 7 (amino acid transporter light chain, L system), member 8	−1.75	[a]
SMG5	23381	Smg-5 homolog, nonsense-mediated mRNA decay factor (*C elegans*)	−1.81	[a]
SNX12	29934	Sorting nexin 12	−3.38	[a]
SYS1	90196	SYS1 Golgi-localized integral membrane protein homolog (*S cerevisiae*)	−1.55	[a]

Supplementary Table 3. Continued

Symbol	ID	Name	Fold change	*P*
TAF15	8148	TAF15 RNA polymerase II, TATA box binding protein (TBP)-associated factor, 68 kilodaltons	−1.72	[a]
TBC1D17	79735	TBC1 domain family, member 17	−1.56	[b]
TBPL1	9519	TBP-like 1	−1.63	[a]
TFAP2C	7022	Transcription factor AP-2 γ (activating enhancer binding protein 2 γ)	−1.59	[a]
TGOLN2	10618	Trans-golgi network protein 2	−1.96	[a]
TMEM135	65084	Transmembrane protein 135	−1.52	[a]
TMEM245	23731	Transmembrane protein 245	−1.53	[a]
TMEM161B	153396	Transmembrane protein 161B	−2.25	[a]
TMTC4	84899	Transmembrane and tetratricopeptide repeat containing 4	−2.18	[a]
TPP1	1200	Tripeptidyl peptidase I	−2.83	[a]
UBE2B	7320	Ubiquitin-conjugating enzyme E2B	−1.94	[a]
UBE2H	7328	Ubiquitin-conjugating enzyme E2H	−1.99	[a]
USP3	9960	Ubiquitin-specific peptidase 3	−1.55	[a]
VAMP5	10791	Vesicle-associated membrane protein 5	−1.62	[a]

C elegans, caenorhabditis elegans; S cerevisiae, saccharomyces cerevisiae; S pombe, saccharomyces pombe.
[a] $P < .001$ in comparison with control (miR-scramble)-treated cells.
[b] $P < .01$.